Winter mesoscale circulation on the shelf slope region of the southern Drake Passage

Meng Zhou [a,*], Yiwu Zhu [a], Christopher I. Measures [b], Mariko Hatta [b], Matthew A. Charette [c], Sarah T. Gille [d], Marina Frants [d], Mingshun Jiang [a], B. Greg Mitchell [d]

[a] *The University of Massachusetts Boston, Boston, MA 02125*

[b] *The University of Hawaii at Manoa, Honolulu, HI 96822*

[c] *Woods Hole Oceanographic Institution, Woods Hole, MA 02543*

[d] *Scripps Institution of Oceanography, La Jolla, CA 92093*

[*] Corresponding author. Department of Environmental, Earth and Ocean Sciences, University of Massachusetts Boston, 100 Morrissey Boulevard, Boston, MA 02125, USA.
Tel: +1-617-287-7419; fax: +1-617-287-7474.
E-mail address: meng.zhou@umb.edu

Abstract

An austral winter cruise in July-August 2006 was conducted to study the winter circulation and iron delivery processes in the Southern Drake Passage and Bransfield Strait. Results from current and hydrographic measurements revealed a circulation pattern similar to that of the austral summer season observed in previous studies: The Shackleton Transverse Ridge (STR) in the southern Drake Passage blocks a part of the eastward Antarctic Circumpolar Current (ACC) which forces the ACC to detour southward, produces a Taylor Column over the STR, and forms an ACC jet within the Shackleton Gap, a deep channel between the STR and the shelf of Elephant Island. Observations show that to the west of the STR, the Upper Circumpolar Deep Water (UCDW) intruded onto the shelf around the South Shetland Islands while to the east of the STR, shelf waters were transported off the northern shelf of Elephant Island. Along a similar west-east transect approximately 50 km off the shelf, the northward transport of shelf waters was approximately 2.4 and 1.2 Sv in the austral winter and summer, respectively. The waters around Elephant Island primarily consist of the UCDW that has been modified by local cooling and freshening, unmodified UCDW that has recently intruded onto the shelf, and Bransfield Current water that is a mixture of shelf and Bransfield Strait waters. Weddell Sea outflows were observed which affect the hydrography and circulation in the Bransfield Strait and indirectly affect the circulation patterns in the southern Drake Passage and around Elephant Island. Two Fe enrichment and transport mechanisms are proposed that intrusions of the UCDW onto the northern shelf region of the South Shetland Islands is considered as the results of Ekman pumping due to prevailing westerly wind in the region while the offshelf transport of shelf waters in the shelf region east of Elephant Island is due to acquisition of positive vorticity by shelf waters from horizontal mixing with onshelf intruded ACC waters.

Key Words: Southern Ocean; Drake Passage, Antarctic Circumpolar Current; shelf waters; mesoscale eddies; mixing; iron transport

1. Introduction

The region including the shelves and straits of the western Antarctic Peninsula, southern Drake Passage and southern Scotia Sea hosts a number of biogeochemical hot spots that support primary producers, krill, and higher trophic level predators (Huntley et al., 1991; Holm-Hansen et al., 1997; Martin et al., 1990b; Hofmann et al., 2004; Ducklow et al., 2007; Hopkinson et al. 2007; Nowacek et al., 2011). The water masses in this region include Antarctic Circumpolar Current (ACC) waters (Antarctic Surface Water, ASW; winter water, WW; and Circumpolar Deep Water, CDW), shelf waters originating from the ACC waters but modified by local cooling and precipitation, Bransfield Basin waters originating from Weddell Sea and further locally cooled, and Weddell Sea slope and basin waters (Nowlin and Klinck, 1986; Orsi et al., 1995; Hoffmann et al., 1996; Gordon et al., 2000; Schodlok et al., 2002; Garabato et al., 2002; Brandon et al., 2004; Heywood et al., 2004; Frants, et al., this volume). Onshelf intrusions of the warm CDW are an important mechanism for heat transport onto shelf regions of the western Antarctic Peninsula, and they affect both biological activities and ice dynamics (Klinck, 1998; Zhou et al., 2002, 2006; Martinson et al., 2008). Offshelf transport of iron (Fe)-rich shelf waters fertilizes the southern Scotia Sea region at a horizontal scale of 1000 km (Hopkinson et al. 2007; Zhou et al. 2010, Measures et al., this volume). The physical processes that drive onshelf intrusions of CDW and offshelf transport of shelf waters are fundamental drivers of ecosystem processes and determine the productivity in this region.

The mechanisms that govern onshelf intrusions of the CDW have been studied by several groups in the last several decades (Niiler et al., 1991; Orsi et al., 1995; Hoffmann et al., 1996; Amos, A.F., 2001; Martinson et al., 2008). Hydrographic measurements have provided ample evidence that onshelf intrusions of the CDW occur mostly within deep canyons showing topographic

control (Klinck, 1998; Dinniman et al., 2004; Klinck et al. 2004). It has been hypothesized that the intrusions of shelfbreak currents onto shelves are associated with the curvature of a shelf break or the presence of deep troughs (Dinniman et al., 2004). However, the dynamics driving such intrusions remains uncertain.

The offshelf transport of shelf waters north of Elephant Island has been attributed to the interaction between a topographically-steered branch of the ACC and the shelf waters around Elephant Island (Orsi et al., 1995; Amos, 2001; Schodlok et al., 2002; Zhou et al., 2010; Frants et al., this volume-a). A portion of the ACC is blocked by the Shackleton Transverse Ridge (STR), which rises from an ocean basin of deeper than 4000 m to closer than 800 m to sea surface, and is 20 km wide and 200 km long (Fig. 1). The southern boundary of the ACC is steered to the south by the ridge crossing the narrow Shackleton Gap between Elephant Island and the STR forming a jet of 60 cm s^{-1} and a Taylor column (a standing eddy) over the ridge. After passing through the Shackleton Gap, which is approximately 3000 m deep and 30 km wide, the majority of this jet is steered northward along the STR, rejoining the main ACC at 59°S. This pathway is consistent with an assumption that potential vorticity is conserved along streamlines. This jet produces a series of mesoscale eddies which translate northeastward, and these carry an offshelf transport of shelf waters northeast of Elephant Island. This offshelf transport is supported by the shelf waters and Bransfield Current, which flows along the shelf break south of the South Shetland Islands and exits between Elephant and Clarence Islands (Zhou et al., 2006, 2010; Frants et al., this volume-a). The ^{224}Ra distribution, a naturally occurring tracer of coastal water masses, also confirmed the rapid advection of shelf waters into the offshelf area north of Elephant Island (Dulaiova et al., 2009).

Numerous studies have indicated that Fe supply is a primary control on phytoplankton biomass

and productivity in the Southern Ocean (Martin et al., 1990a; 1990b; Sedwick and DiTullio, 1997; Boyd et al., 2000; Strutton et al., 2000; Fitzwater et al., 2000; Buesseler et al., 2004; Coale et al., 2004; Holm-Hansen et al., 2004; Hopkinson et al., 2007). In several locations, Fe–limited ACC surface waters are enriched by additions of Fe from shelf waters resulting in significant downstream enhancement of primary productivity (Blain et al., 2007; Hopkinson et al., 2007; Pollard et al., 2007, 2009; Dulaiova et al., 2009; Zhou et al., 2010; Measures et al., this volume). The naturally added Fe is delivered either by vertical and horizontal mixing (Blain et al., 2007; Charette et al., 2007; Pollard et al., 2007; Park et al., 2008; Frants et al., this volume-b), or horizontal transport (Dulaiova et al., 2009; Zhou et al., 2012; Frants et al., this volume-b). On the Kerguelen Plateau in the Southern Ocean, a large phytoplankton bloom was found to be sustained by Fe and macronutrient–rich deep waters supplied to the euphotic zone through vertical mixing (Blain et al., 2007). In the CROZEX study, the island/plateau–derived Fe flux from horizontal mixing was estimated to be 3–6 times larger than the vertical supply (Charette et al., 2007). In the southern Drake Passage, the Fe–rich water derived from the shelf north of Elephant Island fertilizes the southern Scotia Sea at a horizontal scale of 100-1000s km (Dulaiova et al., 2009; Hatta, et al., this volume; Measures, et al., this volume).

The mixing between the Fe-poor ACC waters and Fe-rich shelf waters downstream of the STR leads to strong gradients within chemical and biological variables, including nutrients, chlorophyll and zooplankton (Huntley et al., 1991; Holm–Hansen et al., 2004; Hopkinson et al., 2007; Kahru et al., 2007; Hewes et al., 2008, 2009; Reiss et al., 2009). Corresponding to the primary features at the STR, the southward-deflected ACC branch and the mesoscale eddies in the leeside of the STR, the Fe-rich waters on the shelf originate from Fe-poor UCDW waters that intrude onto the shelf and then are enriched by Fe on the shelf (Hatta, et al., this volume;

Measures, et al., this volume). Among these waters, seasonal heating and cooling affect not only the surface properties but also the strength and meridional location of the ACC (Sprintall, 2003). Long term observations crossing the Drake Passage show that the mean transport and standard variation between 59°S and 61°S are approximately 5 and 15 $m^3 s^{-1}$ per m in the latitude, respectively. To observe the seasonal changes in circulation patterns and associated water masses between summer and winter and to understand the driving mechanisms for on-shelf and offshelf transport were the primary objectives of the 2006 winter cruise described herein.

2. Data and methods

The austral winter cruise was conducted from July 3 to August 15 2006 around the STR onboard the I.B.R.V. Nathanial B. Palmer. The study area in the Southern Drake Passage is bounded between 60°S and 65°S and 64°W and 53°W (Fig. 1). Two basins deeper than 4000 m are divided by the northwest-southeast STR, and linked by the Shackleton gap deeper than 3000 m located between the STR and the shelf break northwest of Elephant Island. The shelves around the South Shetland and Elephant Islands have sharp shelf slopes, and separate those deep basins in the southern Drake Passage from the Bransfield Strait. The large scale spatial survey and long transects in the 2006 cruise were designed to resolve the circulation patterns and water masses in the study area. In the shelf break regions, additional stations were added to resolve fronts and jets. The austral summer cruise in 2004 was conducted in the same region using the similar survey strategies and details can be found in Zhou et al. (2006, 2010).

Two rosette systems were used in both 2004 and 2006 cruises, a regular rosette system equipped with a SeaBird 911 plus conductivity–temperature–depth (CTD) system including dual

temperature and conductivity sensors (Sea-Bird Electronics, Inc., Bellevue, WA, USA), and a trace metal clean rosette with a SeaBird 911 plus CTD system including one pair of temperature and conductivity sensors. All temperature and conductivity sensors were calibrated prior to the cruises to the standard initial accuracies of 0.001ºC and 0.003 mmho cm^{-1}, respectively. Discrete samples for salinity analysis were drawn from the rosette Niskin bottles to ensure the stability of these conductivity sensors. All CTD casts were to depths of 1000 m or 10 m above the bottom when the depth was less than 1000 m. All CTD data were processed by applying filters and corrections suggested by Sea-Bird Electronics, Inc., and the resulting data were binned to 1 m intervals. The standard deviations between the paired temperature and salinity sensors on the SeaBird 911 plus CTD system in 1 m bins were all within 0.01ºC and 0.01, respectively.

Both the A.S.R.V. Laurence M. Gould and I.B.R.V. Nathanial B. Palmer were mounted with a vessel-mounted (VM) 153 kHz Narrow Band (NB) Acoustic Doppler Current Profiler (ADCP) (RD Instruments, San Diego, CA, USA), and were used for the direct current measurements. Both the ADCPs were set with a bin length of 8 m, a pulse length of 8 m, and a blank after transmission of 4 m. These settings lead to a standard deviation of 13 cm s^{-1} for single ping measurements (RDI, 1989). A 15–minute ensemble average is made for the velocity measurements, which reduces the corresponding error to approximately 0.6 cm s^{-1}.

In situ ADCP measurements include tidal current with the time scale of tens of hours, and wind driven currents and mesoscale eddies on the time scale of several days during the study period. Spatial and temporal variability associated with tides, wind and eddies would bias current maps generated from the ADCP survey. To study the current field in a specific region, the survey was carried out over a 3-7 day period. For example the 3 west-east transects north of Elephant Island were carried out over 7 days between July 17 and 23, 2006. To obtain geostrophic currents, we

need to remove tidal currents based on a tidal current model for the Antarctic shelves (Padman et al., 2002), and then to fit the detided current data with a streamfunction (Bretherton et al., 1976; Dorland and Zhou, 2007). Because there is no geostrophic streamfunction associated with either tidal or wind driven currents, fitting a geostrophic streamfunction to detided currents during interpolation will further remove ageostrophic components from current measurements to provide better geostrophic current estimates. These interpolations were unquestionably biased by the limited spatial and temporal data coverage in our study area. However, the streamfunction fitting is expected to help us to remove random small-mesoscale variations and also random ship tracks in order to provide a view of the large-scale pattern. In particular, the consistency between current patterns and hydrographic fields provides additional confidence in the large-scale circulation patterns.

3. Results

The spatial distribution of potential temperature (θ) and salinity (S) are shown in Fig. 2. The ACC surface water at 20 m was the warmest and freshest with θ (~ -0.4°C) and S (<33.9). On the shelves the surface water was cooler and saltier, since it was affected by surface cooling and mixing between waters from the ACC and Bransfield Strait. The surface water found in the Bransfield Strait, especially near the western Antarctic Peninsula, was the coldest and saltiest with θ (~ -1.8°C) and S (~34.5). At 200 m, the CDW in the ACC region was the warmest and saltiest with θ (~1.5°C) and S (~ 34.5). This water is below a surface mixed layer, which is approximately 100 m deep (Fig. 3). The upper mixed layers on shelves and in the Bransfield Strait were as deep as 400-500 m. The offshelf transport of the waters from shelves and the

Bransfield Strait can be seen from the θ–S characteristics in the shelf slope region north of Elephant Island at both 20 and 200 m.

The θ–S characteristics of the entire study area were mostly bounded by the θ–S curves of the ACC region and the Weddell Sea with an exception of the deep water in the Bransfield Strait basin, which originates from the Weddell Sea but is significantly cooled locally (Fig. 3). In the vertical the surface water was the coolest as a result of winter cooling, and the CDW was the warmest. In the horizontal, the CDW in the ACC was the warmest and the surface water of the Weddell Sea was the coolest. In the offshelf area north of Elephant Island, the θ–S characteristics were bounded by those of the ACC (red line) and shelf waters (pink line) found on the northern shelf of Elephant Island.

The currents at 103 and 199 m in the shelf and offshelf regions around Elephant Island from the 2004 austral summer cruise are shown in Fig. 4 for comparison with the current fields from the 2006 austral winter cruise (Figs. 5 and 6). The details of the 2004 cruise can be found in Zhou et al. (2006, 2010). These two depths are chosen to avoid wind driven currents and oscillations, which are surface-intensified. The ACC formed a Taylor Column, a topographically steered large eddy over the STR. Eddies and offshelf transport occurred in the shelf slope region north of Elephant Island. Previous work by the World Ocean Circulation Experiment (WOCE) Standard Surface Velocity Program (SVP) drifters showed that the Bransfield Current flowed along the shelf slope south of the South Shetland Islands, exited between Elephant and Clarence Islands, and flowed off the shelf north of Elephant Island (Zhou et al., 2006, 2010).

The current field at 104 m for the entire 2006 austral winter study area is shown in Fig. 5, and the current fields at 104 and 200 m in the enlarged area around Elephant Island are shown in Fig. 6.

The ACC had a southward component, which might lead to ACC intrusions onto the shelves of the western Antarctic Peninsula. The Taylor Column associated with the STR can be seen clearly while eddies and offshelf transport occurred in the shelf slope region north of Elephant Island. In the Bransfield Strait, the southwestward current can be seen along the northern shelf slope of the western Antarctic Peninsula (Fig. 5); a northeastward current in the Gerlache Strait into the western Bransfield Strait; and an eastward Bransfield Current, along the southern shelf slope of the South Shetland Islands. The Bransfield Current was not as uniform as seen in the austral summer but still exited the Bransfield Strait between Elephant and Clarence Islands.

The horizontal and vertical distributions of water masses are shown in Fig. 7. The penetration of the warm CDW was limited by the northern shelf slope of the South Shetland Islands, while small parcels of onshelf intruding CDW can be seen in the temperature and salinity anomalies on the shelf. The Weddell Sea deep water (WSDW) originates from CDW with a similar salinity but cooler temperature due to heat loss (Fig. 7 EBT). The Weddell Sea shelf break current can be seen from the low temperature and salinity centers marked by "SBC" on Transect EBT near the 1000 m isobath similar to that of the Antarctic Slope Front (Gill, 1973; Heywood et al., 2004; Thompson et al., 2009). Along the shelf slope north of South Shetland and Elephant Islands, the upwelling can be seen on the MBT and WBT where the deep water was raised along the slope marked by H_1 and H_2, and the offshelf transported low temperature and low salinity shelf waters can be seen along this transect in the area off the shelf north of Elephant Island.

The θ–S properties on transect b-b show the separation between the ACC and shelf waters at the STR (Fig. 8). On this transect, the winter mixed-layer depth was approximately 100 m. Within the surface mixed layer the water was cold and fresh due to winter surface cooling and precipitation. At depth, the Upper CDW (UCDW) was the warmest in our study region reaching

approximately 2°C at 500 m. In the shelf water region the shelf water occupied the weakly stratified upper layer of 700-800 m, and was found above the Lower CDW (LCDW). The geostrophic current estimates relative to 1000 m in the north-south directions perpendicular to the CTD transect and the north-south component of the ADCP current measurements exhibit similar positions of fronts and mesoscale eddies. The maximum geostrophic current relative to 1000 m is associated with the front between the ACC and shelf waters which reaches 25 cm s^{-1}, while the direct ADCP current measurements show values of approximately 50 cm s^{-1}.

Two similar CTD transects in Fig. 9 show that the ACC intrusion over the STR extended further east less mixed with the shelf waters during the austral summer 2004 than the ACC did during austral winter 2006. In austral summer 2004 the ACC waters intruded to 55°W far beyond the STR which is at 56°20'W, and the geostrophic current estimates relative to 1000 m were less than 10 cm s^{-1}. In contrast during the austral winter 2006, the ACC waters arrived only at the STR, but the geostrophic current estimate relative to 1000 m reached approximately 20 cm s^{-1}. The off-shelf transport relative to 1000 m in austral winter 2006 was 2.4 Sv twice that of the1.2 Sv seen during austral summer 2004.

The offshelf extension of the shelf waters is shown in Fig. 10. At the SG, shelf waters were limited from transporting northward by the ACC. As the ACC core turned northward after the STR, shelf waters were transported off the shelf and occupied approximately the upper 800 m of the water column along transects 1, 3 and 5 and the upper 400 m along transects 7 and 9. However, the shelf waters at transects 1, 3 and 5 did not extend as far offshore as that of transects 7 and 9 and were confined to a narrower upper layer of 200-300 m by the presence of CDW. In contrast the shelf waters at transects 7 and 9 extended father off the shelf and were

confined within an upper 400 m layer. Some mesoscale horizontal mixing and exchanges between the ACC and shelf waters can be easily seen in these transects.

4. Discussion

4.1. Distribution of water masses

The waters in the study area are generally bounded between the warmer CDW in the ACC region and cooler waters of the modified CDW in the shelf, Bransfield Strait and Weddell Sea regions (Figs. 2 and 3). Because the Weddell Sea is cold and saline, the potential densities of surface waters there are similar to that of the UCDW below 200 m. Thus, the Weddell Sea deep water at the slope and basin regions exits the Weddell Sea further east of our study area following the 1000 m isobath, and subducts due to its density beneath the UCDW deeper than 200 m in the ACC region (Heywood et al., 2004). Because these Weddell Sea surface and deep waters are below the surface euphotic zone, they will be below will not therefore directly support Fe fertilization processes in the euphotic zone till they are vertically upwelled or mixed.

The water masses around the Elephant Island region are contributed to by different sources: the original shelf waters of the South Shetland Islands and Elephant Island, the Bransfield Current, on-shelf intruded ACC waters, and Weddell Sea waters from its shelf and slope (Zhou et al., 2010; Frants et al., this volume). The Weddell Sea waters originate from the CDW and are significantly cooler and saltier than waters originating from the South Shetland Islands and Elephant Island (Fig. 2). Though the Bransfield Strait waters also originate from the Weddell Sea, their θ-S characteristics are modified significantly by local processes (Nowlin and Klinck, 1986; Orsi et al., 1995; Hoffmann et al., 1996; Gordon et al., 2000). The Bransfield Current is

surface-intensified as implied by the tilted isopycnals in Transect MBT (Fig. 7), carries waters primarily from the shelves within the upper layer of 500-600 m (Zhou et al., 2006), and exits between Elephant and Clarence Islands. The exiting waters are primarily composed of the shelf waters in the upper 500-600 m and Bransfield Strait deep water in the lower layer (Fig. 3).

Different shelf waters may experience different Fe enrichment processes as indicated by the results of the trace metal determinations (Hatta et al., this volume; Measures et al., this volume). The stronger onshelf intrusions of the UCDW and wave action along the northern shelf of the South Shetland and Elephant Islands may produce stronger sediment resuspension and greater pore water fluxes into the overlying water column. Such a Fe supply mechanism is supported by observed trace metal concentrations and optical transmittance which show a plume of elevated Al, Fe and Mn concentrations co-occurring with the maximum in resuspension. If the winter deep mixed layer extends to 500 m, the shelf areas shallower than 500 m will be a major Fe source to the surface water during the winter season. In the summer, seasonal stratification reduces the surface mixed layer depth to approximately 50 m (Zhou et al., 2010). Seasonal stratification will not only significantly reduce vertical mixing, but will also the limit the surface water to being in contact with sediment only from shelf areas that are shallower than 50 m. The higher ratio of dissolved Fe to manganese in the winter implies stronger sediment resuspension due to stronger vertical mixing as compared to results obtained during the summer cruise. The offshelf transport of Fe in the stratified water column during the summer season can be considered as the minimum (~2.8×10^6 mole Fe yr^{-1} in the upper 100 m based on the 2004 summer cruise) due to weakest sediment resuspension limited by stratification while the offshelf transport of Fe in the mixed water column during the winter can be considered as the maximum (~5.0×10^7 moles Fe yr^{-1} in the upper 100 m based on the 2006 winter cruise) due to strongest

vertical mixing by wave actions and convection. However considering the mesoscale variations of circulation and Fe fields and our values based only on 2 cruises, more field process and monitoring studies are needed for estimating seasonal means and variations of offshelf transport of Fe in this study region.

4.2. Onshelf intrusions of ACC waters

Onshelf intrusion of the CDW is a critical physical mechanism not only for transporting heat onto the shelf regions in the western Antarctic Peninsula, but also being the source water that is enriched in iron on the shelves and then transported off the shelves. The westerly wind in the ACC region produces an upwelling at the shelf slope, which can be seen from the upward shoaling isopycnals in Transects WBT and MBT in Fig. 7. The upwelled warm UCDW intrudes onto the shelf of the South Shetland Islands from beneath the cold upper surface layer. The surface slope in the offshelf direction associated with the density gradient produces a barotropic northeastward geostrophic current along the shelf slope, a feature that is also observed in numerical modeling studies (Dinniman and Klinck, 2004). Onshelf intrusions of the UCDW are interpreted as indicating that the along shelfbreak current is topographically steered by the curvature of a shelfbreak. However if the current along a shelfbreak is governed by the conservation of potential vorticity, intrusions that cross isobaths onto shelves will require changes in potential vorticity. Here we provide an alternative mechanism. As a westerly wind in the ACC region produces an upwelling at the shelf slope, the UCDW is vertically stretched by upwelling while being advected eastward along the shelf slope. Based on the potential vorticity conservation (e.g. Pedlosky, 1987), the vertical stretching of the UCDW by Ekman pumping can be written as,

$$\frac{d}{dt}\left(\zeta + f + |f|\frac{\delta H}{H}\right) = \left.\frac{d\zeta}{dt}\right|_a, \quad (1)$$

where ζ is the relative vorticity, f is the Coriolis constant, δH is the change of the layer thickness (H), and $d\zeta/dt|_a$ is a notation of vorticity addition produced by Ekman pumping. We also assume that the relative vorticity is much smaller than the planetary vorticity. The vorticity can be produced by Ekman pumping, i.e.,

$$\left.\frac{d\zeta}{dt}\right|_a = f\nabla\cdot\mathbf{u}_a, \quad (2)$$

where $\mathbf{u}_a$ is the wind driven current (Pedlosky, 1987). Combining Eqs (1) and (2), we have

$$\frac{d}{dt}\left(\zeta + f + |f|\frac{\delta H}{H}\right) = f\nabla\cdot\mathbf{u}_a. \quad (3)$$

The divergence produced by Ekman pumping leads to an increase in negative relative vorticity in the Southern Hemisphere that rotates the along-slope geostrophic current from the northeastward to the southward onto the shelf. Assuming that the onshelf intrusion of the UCDW stops when the Ekman pumping is balanced by the squeezing of the water column due to the decrease in bottom depth, from Eq. 3 we will have

$$\frac{d}{dt}\left(\frac{\delta H}{H}\right) = \frac{f}{|f|}\nabla\cdot\mathbf{u}_a. \quad (4)$$

Note the total layer thickness change (ΔH) from H_1 to H_2 as integrating δH in the period (t_w) of an upwelling wind event (Fig. 7). Integrating Eq. 4, we have

$$\frac{\Delta H}{H} = -t_w \nabla \cdot \mathbf{u}_a , \tag{5}$$

where $f/|f| = -1$ in the Southern Hemisphere. Therefore, an upwelling event will lead to a negative change in relative vorticity for the onshelf intruding layer. Assuming the wind stress (τ) can be written as (Smith, 1988),

$$\tau = 0.002 \rho_a W^2 \tag{6}$$

where ρ_a is air density, W is the wind speed and a drag coefficient of 0.002 is chosen to be roughly consistent with published values which vary from 0.0012 at low latitudes to 0.0016 at high latitudes (Trenberth etal., 1989). The mean velocity in the Ekman layer is

$$u_a = \frac{0.002 \rho_a W^2}{\rho M |f|}, \tag{7}$$

where u_a is the magnitude of $\mathbf{u}_a$, ρ is the water density, and M is the mixed-layer depth. We also assume that the divergence $\nabla \cdot \mathbf{u}_a$ can be substituted by u_a / R_i, where R_i is the width of a shelf slope upwelling area. Combining Eqs. 5 and 7, we have

$$\frac{H_2}{H_1} = 1 - \frac{0.002 t_w \rho_a W^2}{\rho M R_i |f|}. \tag{8}$$

The relationships between the ratio of the shelf bottom depth (H_2) to upwelling depth (H_1), wind speed and wind event duration are shown in Fig. 11 where we assume M, R_i, f and ρ_a are equal to 100 m, 100 km, 10^{-4} s^{-1}, and 1.2 kg m^{-3}, respectively. The intrusions of the UCDW onto shelves require significant wind energy. For example, given a wind event of 14 m s^{-1} for a period of 2.8 days, the UCDW at the depth of 500 m can be stretched by an upwelling to intrude onto a shelf

depth of 400 m. Thus, the prevailing westerly wind in the ACC region produces the upwelling at the northern shelf slope of the South Shetland Island; the negative vorticity provided by Ekman pumping leads to on-shelf intrusion of the UCDW; and the intruding depth change of the UCDW is dependent on the wind speed and duration. Note that the relationship in Eq. 8 and Fig. 10 is theoretical for understanding physical mechanisms where M and R_i are hypothetical and can be significantly different from real values. Considering the wind field varies seasonally, annually and also on the climate scale, this relationship indicates that onshelf intrusions of the UCDW will change accordingly, that will also affect the Fe enrichment process of the UCDW on shelves.

4.3. Topographic steering and offshelf transport

The topographic blockage of the STR to the ACC produces the southward intrusion of the ACC, a Taylor Column over the STR and a jet within the Shackleton Gap (Zhou et al., 2010). The offshelf transport of shelf waters was found on the downstream side, north of Elephant Island during both austral summer and winter (Figs. 4, 6 and 9). The relationship between the northward-turned ACC jet at the downstream side of the STR and offshelf transport of shelf waters north of Elephant Island is still not known. Such interactions between a major offshelf jet and shelf waters are frequently seen such as the separation of the Gulf Stream from the shelfbreak at Cape Hatteras together with the offshelf transport of the Mid-Atlantic and South-Atlantic Bight waters (Savidge and Bane Jr, 2001), and the separation of the coastal upwelling jet as a part of the California Current System at Cape Blanco (Barth et al., 2000). The driving mechanisms for the separation of shelf slope jets in the offshelf direction have been explored as the blockage of shelf waters or Ekman transport convergence.

The offshelf transport north of Elephant Island occurs over depths down to 500-800 m (Fig. 10),

which cannot simply be explained by blockage or surface Ekman layer dynamics. Here we provide a horizontal mixing mechanism between the ACC and shelf waters illustrated in Fig. 12. It is clear that a branch of ACC waters is detoured southward by the blockage of the STR. The vorticity conservation equation can be written as,

$$\Delta\zeta = -\beta\Delta y - |f|\frac{\Delta H}{H}. \tag{9}$$

where $\Delta\zeta$, Δy and ΔH are the relative vorticity acquired, latitude change and depth layer change, respectively. The ACC waters acquire a positive vorticity because both Δy and ΔH are negative as the ACC branch moves southward and is squeezed by the shallow shelf. A part of the ACC waters intrudes on to the shelf of Elephant Island, and is mixed with shelf waters as clearly seen in Figs. 9 and 10. The horizontal mixing of ACC waters with shelf waters provides a positive vorticity to the shelf waters around Elephant Island. If the layer thickness of shelf waters changes, the relative vorticity (ζ_S) of the layer can be written as,

$$\frac{d}{dt}(\zeta_S + \beta y) = K\nabla^2\zeta_S. \tag{10}$$

where K is the horizontal mixing coefficient. Expanding the left side and neglecting the local change of relative vorticity, we have

$$v\beta = K\nabla^2\zeta_S. \tag{11}$$

where v is the northward velocity component. Integrating Eq. 11 over an area (A) of shelf waters on a shelf, we have

$$V_A = \frac{K}{A\beta}\iint_A \nabla^2 \zeta_S \, dA \,. \tag{12}$$

where V_A is the mean northward velocity in the area (A). Applying Ostrogradsky's divergence theorem (Riley et al., 2010) to Eq. 12, we have

$$V_A = \frac{K}{A\beta}\oint_L (\nabla \zeta_S \cdot \mathbf{n}) dL \,. \tag{13}$$

where L is the boundary of A, $\mathbf{n}$ is the outward pointing unit normal field of the boundary L. Because the southward intruded ACC waters acquire a positive vorticity (Eq. 9), Eq. 12 implies that the positive vorticity acquired by shelf waters due to horizontal mixing with ACC waters naturally leads to a northward transport of shelf waters by the β effect. A stronger mixing between the ACC and shelf waters will lead to a stronger northward offshelf transport. Because the on-shelf intrusions of the UCDW are pulsing events, we expect that offshelf transport also occurs in pulses related to onshelf intrusion events. The mesoscale eddies and mixture of waters downstream of the STR provides the physical evidence (Zhou et al., 2010). The estimates of radium isotope ages also provide independent evidence of rapid offshelf transport of shelf waters in the STR region (Dulaiova et al., 2009).

4.4. Seasonal variations

A comparison of the front between the ACC and shelf waters is shown in Fig. 9. The front extended further to the east in the austral summer than in the austral winter while the horizontal mixing was stronger in austral winter 2006 than in austral summer 2004. The offshelf transport in austral winter 2006 was twice that of austral summer 2004. As suggested by Eq. 12, a stronger horizontal mixing between ACC and shelf waters in austral winter 2006 could lead to a

stronger offshelf transport of shelf waters. The offshelf transport estimates should include a mixture between the ACC and shelf waters. The stronger winter horizontal mixing as discussed in the previous section can be interpreted as a result of the stronger westerly winds during austral winter that contributed to a stronger ACC and onshelf transport of the UCDW. It is important to note that these results are based on the data collected during the survey periods, and therefore do not reflect the statistical mean of a season.

The depth at the edge of shelves around the South Shetland, Elephant and Clarence Islands begins at approximately 500 m. Thus, the interaction between the ACC and shelf waters originates from this depth, and the primary onshelf intruding waters are the UCDW. Winter cooling produces the cold surface layer while the freshwater from precipitation keeps the water column weakly stratified. With strong ACC currents intruding onto the shelves, the Fe-rich waters near the bottom can be stirred and mixed upward. The overall stratification in the austral winter is significantly weaker than that of the austral summer due to the surface cooling and that implies stronger vertical mixing fluxes of nutrients. These nutrients, including micronutrients such as Fe, would be available in high concentration at the transition from winter to spring, and therefore may control the intensity and spatial extent of the spring phytoplankton bloom.

5. Summary

The circulation pattern during the austral winter 2006 in the southern Drake Passage was similar to that of the austral summer 2004. The blockage by the STR leads to a branch of the ACC detouring southward, and the formation of a Taylor Column over the STR and a jet within the Shackleton Gap between the STR and the northern shelf of Elephant Island. The consistency

between the austral summer and winter circulation patterns implies that the primary forcing is the blockage by the STR of the ACC in the Southern Drake Passage. The Weddell Sea outflow is complicated, consisting of shelf currents, a shelf break current and Weddell Sea Deep Waters, which may directly affect the circulation in the Bransfield Strait and southern Scotia Sea and also indirectly affect the circulation pattern around the STR. The waters transported off the shelf north of Elephant Island are primarily made up of the shelf waters around the South Shetland, Elephant and Clarence Islands, and the waters associated with the Bransfield Current. The Bransfield Current has been considered as a western boundary current driven by deep Sverdrup transport in the Bransfield Strait (Zhou et al., 2006).

Intrusions of the CDW on to the northern shelf around the South Shetland Islands have been suggested to be a result of the acquisition of negative relative vorticity due to stretching of the UCDW water column by surface Ekman pumping that rotates the northeastward flowing ACC to the onshelf direction. The extension of onshelf intrusions, the bottom depth change of an intruding UCDW, is suggested to be a function of wind speed and duration, i.e., a stronger and longer upwelling wind event will lead to a stronger on-shelf intrusion of the UCDW.

Offshelf transport of shelf waters occurs on the northern shelf of Elephant Island, to the east of the STR. The mechanism for a northward offshelf transport has been proposed to be the result of acquiring a positive relative vorticity by shelf waters and the β-effect. Positive vorticity is acquired when the UCDW moves southward due to the blockage by the STR as a result of the β-effect and also squeezing by shelf depth. As the ACC jet is formed within the Shackleton Gap, the majority of this jet turns northward, but some of it intrudes onto the shelf of Elephant Island. Horizontal mixing between shelf waters and onshelf intruding UCDW carrying positive relative

vorticity leads to a northward transport of mixed shelf and UCDW waters as a result of the β-effect.

These two mechanisms indicate that onshelf intrusions of the UCDW and offshelf transport of shelf waters are primarily driven by the strengths of upwelling and the south-detoured ACC branch, both of which are strongly affected by wind fields. Thus, strong seasonal, interannual and climate variations of onshelf intrusions and offshelf transport are expected which will in turn affect Fe enrichment on shelves and offshelf transport of Fe. For better understandings of climate impacts on Southern Ocean ecosystems and carbon export, more studies are needed to have better understandings of these Fe enrichment and transport processes and better estimates of the seasonal, interannuala and climate variations of Fe transport from shelves to the ACC region.

Acknowledgement

This project was supported by the National Science Foundation grant numbers OPP-0229966, ANT-0444040 and ANT-0948378 to M. Zhou, OPP0230445, ANT0443403 and ANT-0948357 to C. Measures, ANT0443869 and ANT-0948442 to M. Charette, and OPP0230443, ANT0444134 and ANT0948338 to B.G. Mitchell. We would like to acknowledge Raytheon Polar Service Co. for assisting with networking, data transferring and CTD casts, and the crews of the A.S.R.V. L.M. Gould and R.V.I.B. N.B. Palmer for tirelessly fighting the rough sea.

References

Amos, A.F., 2001. A decade of oceanographic variability in summertime near Elephant Island, Antarctica. Journal of Geophysical Research, 106, 22401-22423.

Barth, J.A., Pierce, S.D., Smith, R.K., 2000. A separating coastal upwelling jet at Cape Blanco, Oregon and its connection to the California Current System. Deep-Sea Research II 47, 783-810.

Blain, S., B. and 46 others, 2007. Effect of natural iron fertilization on carbon sequestration in the Southern Ocean, Nature, 446, doi:10.1038.

Boyd, P.W. and 32 others, 2000, A mesoscale phytoplankton bloom in the polar Southern Ocean stimulated by iron fertilization. Nature 407, 695-702.

Brandon, M.A., Naganobu, M., Demer, D.A., Chernyshkov, P., Trathan, P.N., Thorpe, S.E., Kameda, T., Berezhinskiy, O.A., Hawker, E.J., Grant, S., 2004. Physical oceanography in the Scotia Sea during the CCAMLR 2000 survey, austral summer 2000. Deep–Sea Research II, 51, 1301-1321.

Bretherton, F.P., Davis, R.E., Fandry, C.B., 1976. A technique for objective analysis and design of oceanographic experiments applied to MODE-73. Deep-Sea Research 23, 559–582.

Buesseler, K.O., Andrews, J.E., Pike, S.M., Charette, M.A., 2004. The effects of iron fertilization on carbon sequestration in the Southern Ocean. Science, 304, 414-417.

Charette, M. A., Gonnee, M. E., Morris, P. J., Statham, P., Fones, G., Planquette, H., Salter, I., Garabato, A. N., 2007, Radium isotopes as tracers of iron sources fueling a Southern

Ocean phytoplankton bloom, Deep-Sea Research II, 54, 18-20.

Coale, K.H. and others, 2004. Southern ocean iron enrichment experiment: Carbon cycling in high- and low-Si waters. Science, 304, 408-414.

Dinniman, M.S., Klinck, J.M., 2004. A model study of circulation and cross shelf exchange on the west Antarctic Peninsula continental shelf. Deep-Sea Research II, 51, 2003–2022.

Dorland, R.D., Zhou, M., 2008, Circulation and heat fluxes during the austral fall in George VI Sound, Antarctic Peninsula, Deep–Sea Research II, 55, 294–308.

Ducklow, H.W., Baker, K., Martinson, D.G, Quetin, L.B., Ross, R.M., Smith, R.C., Stammerjohn, S.E., Vernet, M., Fraser, W., 2007. Marine pelagic ecosystems: the West Antarctic Peninsula. Philosophical Transactions of Royal Society B, 362, 1477 67-94.

Dulaiova, H., Ardelan, M.V., Henderson, P.B., Charette, M. A., 2009. Shelf-derived iron inputs drive biological productivity in the southern Drake Passage. Global Biogeochemical Cycles, 23, GB4014, doi:10.1029/2008GB003406.

Fitzwater, S.E., Johnson, K.S., Gordon, R.M., Coale, K.H., Smith, W.O., 2000. Trace metal concentrations in the Ross Sea and their relationship with nutrients and phytoplankton growth. Deep-Sea Research II, 47, 3159-3179

Frants, M., Gille, S.T., Hewes, C.D., Holm-Hansen, O., Lombrozoa, M. A., Measures, C.I., Mitchell, B. G., Wang, H., Zhou, M., 2012. Optimal Multiparameter Analysis of Source Water Distributions in the Southern Drake Passage, Deep Sea Research II, accepted.

Frants, M., Gille, S.T., Hatta, M., Hiscock, W. T., Kahru, M., Measures, C. I., Zhou, M., 2011.

Analysis of horizontal and vertical processes contributing to natural iron supply in the mixed layer in southern Drake Passage, Deep Sea Research II, accepted.

Garabato, A.C.N., Heywood, K.J., Stevens, D.P., 2002. Modification and pathways of Southern Ocean Deep Waters in the Scotia Sea. Deep-Sea Research I, 49, 681-705.

Gill, A. E., 1973. Circulation and bottom water production in the Weddell Sea. Deep-Sea Research, 20, 111-140.

Gordon, A.L., Mensch, M., Dong, Z., Smethie Jr., W.M., de Bettencourt, J., 2000. Deep and bottom water of the Bransfield Strait eastern and central basins. Journal of Geophysical Research, 105, 11,337–11,346.

Hatta, M., Measures, C.I., Selph, K.E., Zhou, M., Yang, J.J., Hiscock, W.T., 2012. Iron fluxes from the shelf regions near the South Shetland Islands in the Drake Passage during the austral-winter 2006, accepted.

Hewes, C., Reiss, C., Kahru, M., Mitchell, B. and Holm-Hansen, O., 2008. Control of phytoplankton biomass by dilution and mixed layer depth in the western Weddell-Scotia Confluence. Marine Ecology Progress Series, 366, 15-29.

Hewes, C.D., Reiss, C.S., Holm-Hansen, O., 2009. A quantitative analysis of sources for summertime phytoplankton variability over 18 years in the South Shetland Islands (Antarctica) region. Deep–Sea Research I, 56, 1230-1241.

Heywood, K.J., Garabato, A.C.N., Stevens, D.P., Muench, R.D., 2004. On the fate of the Antarctic Slope Front and the origin of the Weddell Front. Journal of Geophysical

Research–Oceans, 109, doi:10.1029/2003JC002053.

Hofmann, E.E., Klinck, J.M., Lascara, C.M., Smith, D.A., 1996. Water mass distribution and circulation west of the Antarctic Peninsula and including Bransfield Strait. In Antarctic Research Series, vol. 70, edited by R. Ross, E. Hofmann and L. Quetin, American Geophysical Union, Washington, D.C., pp. 61-80.

Hofmann, E.E., Wiebe, P.H., Costa, D.P., Torres, J.J., 2004. An overview of the Southern Ocean global ocean ecosystems dynamics program. Deep-Sea Research II 51,1921–1924.

Holm-Hansen, O., Hewes, C.D., Villafañe, V.E., Helbling, E.W., Silva, N., Amos, T., 1997. Distribution of phytoplankton and nutrients in relation to different water masses in the area around Elephant Island, Antarctica. Polar Biology, 18, 145-153.

Holm-Hansen, O., Naganobu, M., Kawaguchi,S., Kameda, T., Sushin, V. A., Krasovski, I., Priddle, J., Korb, R., Brandon, M., Demer, D., Hewitt, R.P., Hewes, C.D., 2004. Factors influencing the distribution, biomass, and productivity of phytoplankton in the Scotia Sea and adjoining waters. Deep-Sea Research II, 51, 1333-1350.

Hopkinson, B.M., Mitchell, B.G., Reynolds, R., Wang, H., Hewes, C., Selph, K., Measures, C.I., Holm-Hansen, O., Barbeau, K., 2007. Iron limitation across chlorophyll gradients in the southern Drake Passage: phytoplankton responses to iron addition and indicators of iron stress. Journal of Limnology and Oceanography, 52, 2540-2554.

Huntley, M.E., Karl, D.M., Niiler, P.P., and Holm-Hansen O., 1991. Research on Antarctic Coastal Ecosystem Rates (RACER): an interdisciplinary field experiment. Deep-Sea Research II, 38, 911-942.

Kahru, M., Mitchell, B.G., Gille, S.T., Hewes, C.D., Holm-Hansen, O., 2007. Eddies enhance biological production in the Weddell-Scotia confluence of the Southern Ocean. Geophysical Research Letters, 34, L14603. DOI, 10.1029/2007GL030430.

Klinck, J.M., 1998. Heat and salt changes on the continental shelf west of the Antarctic Peninsula between January 1993 and January 1994, Journal of Geophysical Research, 103, 7617-7636.

Klinck, J.M., Hofmann, E.E., Beardsley, R.C., Salihoglu, B., Howard, S., 2004. Water mass properties and circulation on the west Antarctic Peninsula continental shelf in austral fall and winter 2001. Deep-Sea Research II, 51, doi:10.1016/j.dsr2.2004.08.001.

Martin, J.H., Gordon, R.M., Fitzwater, S.E., 1990a. Iron in Antarctic waters. Nature, 345, 156-158.

Martin, J.H., Fitzwater, S.E., Gordon, R.M., 1990b. Iron deficiency limits phytoplankton growth in Antarctic waters. Global Biogeochemical Cycles, 4, 5-12.

Martinson, D.G., Stammerjohn, S.E., Smith, R.C., Iannuzzi, R.A., 2008. Palmer, Antarctica, long-term ecological research program first 12 years: physical oceanography, spatio-temporal variability. Deep-Sea Research II., 55: doi: 10.1016/j.dsr2.2008.04.038.

Measures, C.I., Brown, M.T., Selph, K.E., Apprill, A., Zhou, M., 2012. The Influence of Shelf Processes in Delivering Dissolved Iron to the HNLC waters of the Drake Passage, Antarctica, Deep Sea Research II, accepted.

Niiler, P.P., Amos, A.F., Hu, J.-H., 1991. Water masses and 200 m relative geostrophic

circulation in the western Bransfield Strait region. Deep-Sea Research II, 38, 943-959.

Nowacek, D.P., Friedlaender, A.S., Halpin, P.N., Hazen, E.L., Johnston, D.W., et al., 2011. Super-Aggregations of Krill and Humpback Whales in Wilhelmina Bay, Antarctic Peninsula. PLoS ONE 6: e19173. doi:10.1371/journal.pone.0019173.

Nowlin, W.D. Klinck, J.M., 1986. The physics of the Antarctic Circumpolar Current. Reviews of Geophysics, 24, 469-491.

Orsi, A.H., Whitworth, T., Nowlin, W.D., 1995. On the meridional extent and fronts of the Antarctic Circumpolar Current. Deep-Sea Research I, 42, 641-673.

Padman, P., H.A. Fricker, R. Coleman, S. Howard, and L. Erofeeva, 2002. A new tide model for the Antarctic Ice Shelves and Seas. Annals of Glaciology, 34, 247-254.

Pedlosky, J., 1987. Geophysical Fluid Dynamics. Springer-Verlag, New York, 624pp.

Pollard, R., Sanders, R., Lucas, M., Statham, P., 2007. The Crozet Natural Iron Bloom and Export Experiment (CROZEX), Deep-Sea Research II, 54, 1905-1914.

Pollard, R.T. and 33 others, 2009. Southern Ocean deep-water carbon export enhanced by natural iron fertilization. Nature, 457, doi:10.1038/nature07716.

RDI, 1989. Acoustic Doppler Current Profilers. Principles of Operation: a practical primer. RD Instruments, San Diego, 36pp

Reiss, C.S., Hewes, C.D., Holm-Hansen, O., 2009. Trends and relationships between atmospheric tele-connections and Upper Circumpolar Deep Water (UCDW) influence on phytoplankton biomass around Elephant Island, Antarctica. Marine Ecology Progress

Series 377, 51-62.

Riley, K.F., Hobson, M.P., Bence, S.J., 2010. Mathematical methods for physics and engineering. Cambridge University Press, Cambridge, 1362pp.

Savidge, D.K., Bane Jr., J.M., 2011. Wind and gulf stream influences on along-shelf transport and offshelf export at Cape Hatteras, North Carolina. Journal of Geophysical Research 106, 11,505-11527.

Schodlok, M.P., Hellmer, H.H., Beckmann, A., 2002. On the transport, variability and origin of dense water masses crossing the South Scotia Ridge. Deep Sea Research II, 49, 4807-4825.

Sedwick, P. N., DiTullio, G.R., 1997. Regulation of algal blooms in Antarctic shelf waters by the release of iron from melting sea ice. Geophysical Research Letter, 24, 2515-2518.

Sprintall, J., 2003. Seasonal to interannual upper-ocean variability in the Drake Passage. Journal of Marine Research, 61, 27-57.

Smith, S.D., 1988. Coefficients for sea surface wind stress, heat flux, and wind profiles as a function of wind speed and temperature. Journal of Geophysical Research, 93, 15,467-15,472.

Strutton, P. G., Griffiths, F. B., Waters, R. L., Wright, S. W., Bindoff, N. L., 2000. Primary productivity off the coast of East Antarctica (80-150E), January to March 1996. Deep-Sea Research II, 47, 2327-2362.

Thompson, A.F., Heywood, K.J., Thorpe, S.E., Renner, A.H.H., Trasviñ a, A., 2009. Surface

circulation at the tip of theAntarctic Peninsula from drifters. Journal of Physical Oceanography, 39, 3-26.

Trenberth, K.E., Large, W.G., Olson, J.G., 1989. The effective drag coefficient for evaluating wind stress over the oceans. Journal of Climate, 2, 1507-1616.

Zhou, M., Niiler, P.P. Hu, J.-H., 2002. Surface current in the Bransfield and Gerlache Straits measured by surface Lagrangian drifters. Deep-Sea Research I, 46, 267-280.

Zhou, M., Niiler, P.P., Zhu, Y., Dorland, R.D., 2006. The western boundary current in the Bransfield Strait, Antarctica. Deep Sea Research I, 53, 1244–1252.

Zhou, M., Zhu, Y., Dorland, R.D., Measures, C.I., 2010. Dynamics of the current system in the southern Drake Passage, Deep Sea Research I 57, 1039–1048.

Figure captions

Fig. 1. Bathymetry in the southern Drake Passage and stations during the 2006 austral winter cruise. The inserted panel shows the stations during the 2004 austral summer cruise,, depths are in meters. The black dots represent stations occupied during the cruise. The Star (☆) and square box (□) indicate the stations used to represent the end-members of the ACC and shelf waters, and other symbols (◇, × and +) indicate the stations used for water types in Fig. 3. The white straight line marked by a-a in the inserted panel indicates the transect shown in Fig. 9. The abbreviations are Elephant Island (EI), Clarence Island (CI), Shackleton Gap (SG), King George Island (KGI) and Shackleton Transverse Ridge (STR).

Fig. 2. Horizontal distributions of potential temperature (θ) at 20 m (A), salinity (S) at 20 m (B), θ at 200 m (C), and S at 200 m (D). The thin dash lines are the 500 m isobath.

Fig. 3. θ-S diagrams (A), and vertical profiles of θ (B), S (C) and potential density (σ_θ) (D) for the typical water types in the study area, respectively. In panel A, the small black dots are all θ–S pairs in our survey area, color coded solid lines represent the θ-S diagrams and vertical profiles of waters in the ACC shelf, Bransfield Current, Bransfield Strait basin and Weddell Sea basin regions, the dashed lines are the surface σ_θ contours, and the color and gray scales represent the depths of θ-S pairs.

Fig. 4. Circulation field at 103 m (A) and 199 m (B) based on ADCP current measurements during the 2004 austral summer cruise. The current field was interpolated based on the least-squares streamfunction fitting. The Taylor Column is marked by "TC."

Fig. 5. Circulation field at 104 m based on ADCP current measurements during the 2006 austral

winter cruise. The current field was interpolated based on the least-squares streamfunction fitting.

Fig. 6. Circulation field at 104 m (A) and 200 m (B) based on ADCP current measurements during the 2006 austral winter cruise. The current field was interpolated based on the least-squares streamfunction fitting. The black solid lines indicate where the northward transport is estimated from direct ADCP current measurements, and values are the estimates of northward transport in the upper 200 m.

Fig. 7. Locations of the transects showed in Figs. 7-9 (A), and transects of θ (B), S (C) and σ_θ (D) along 3 south-north red lines marked by WBT, EBT and MBT in panel A. In panels B-D, the vertical black lines indicate the locations and depths of CTD casts, and contour intervals are 0.5 °C, 0.2 and 0.05 for θ, S and σ_θ, respectively. In panel A, the blue solid line marked by b-b indicates the location of the transect shown in Fig. 8, and the yellow solid line marked by c-c indicates the location of the transect shown in Fig. 9. In panel C, SBC marks the location of the shelf break current at the Weddell Sea shelf slope.

Fig. 8. Transects of θ, S, σ_θ, geostrophic current estimates relative to 1000 m, west-east (W-E) component of ADCP current measurements, and S-N component of ADCP current measurements along line b-b indicated in Fig. 7. The vertical black lines indicate the locations and depths of CTD casts, contour intervals are 0.5 °C, 0.2, 0.05 and 5 cm s^{-1} for θ, S, σ_θ and currents, respectively, and SG marks the location of the Shacklton Gap.

Fig. 9. Transects of θ, S and geostrophic current estimates relative to 1000 m along lines a-a and c-c in the 2004 and 2006 cruises, respectively. The locations of these transects are shown

in Figs. 1 and 7. The values inserted in the geostrophic current panels are the positive northward transport estimates in Sv within the sections indicated by dashed lines. The vertical black lines indicate the locations and depths of CTD casts and contour intervals are 0.5 °C, 0.2 and 5 cm s^{-1} for θ, S and currents, respectively.

Fig. 10. Transects of θ and S along lines SG and 1-9 shown in the inserted panel during the 2006 cruise. The vertical black lines indicate the locations and depths of CTD casts and contour intervals are 0.5 °C and 0.2 for θ and S, respectively.

Fig. 11. Predicted relationship between the ratio of a shelf bottom depth (H_2) to the original depth (H_1) of upwelled CDW, wind speed and wind duration. The dashed lines show the example of a 14 m s^{-1} wind would take 2.75 days to raise a water mass at 500 m off the shelf break to a shelf bottom depth of 400 m.

Fig. 12. Plan view of a conceptual configuration of the geophysical fluid dynamic processes in the southern Drake Passage: To the west of the STR, a westerly wind event produces upwelling and stretching of water column that leads to intrusions of the CDW onto the shelf; the blockage of the ACC by the STR produces a Taylor Column and the southward detouring of an ACC branch; the ACC waters that intrude onto the shelf acquire a positive vorticity due to the β-effect and are horizontally mixed with shelf waters leading to a northward offshelf transport.

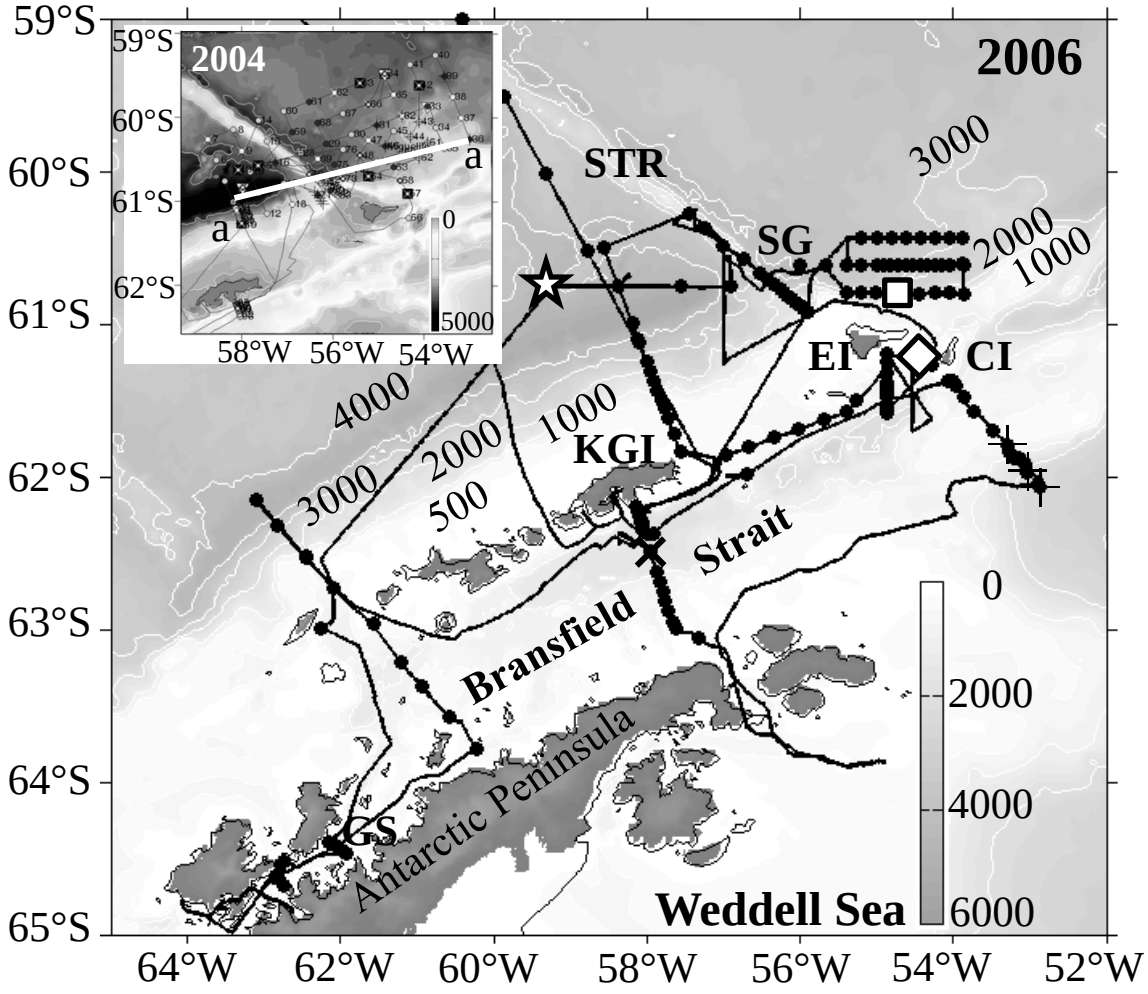

Fig. 1. Bathymetry in the southern Drake Passage and stations in the 2006 austral winter cruise. The inserted panel is the stations in the 2004 austral summer cruise. The depth is in meters. The black dots represent stations occupied during the cruise. The Star (☆) and square box (□) indicate the stations used to represent the endmembers of the ACC and shelf waters, and other signs (◇ , × and +) indicate the stations used for water types in Fig. 3. The white straight line marked by a-a in the inserted panel indicates the transect shown in Fig. 9. The abbreviations are Elephant Island (EI), Clearance Island (CI), Shackleton Gap (SG), King George Island (KGI), Shackleton Transverse Ridge (STR) and Gerlache Strait (GS).

Fig. 01

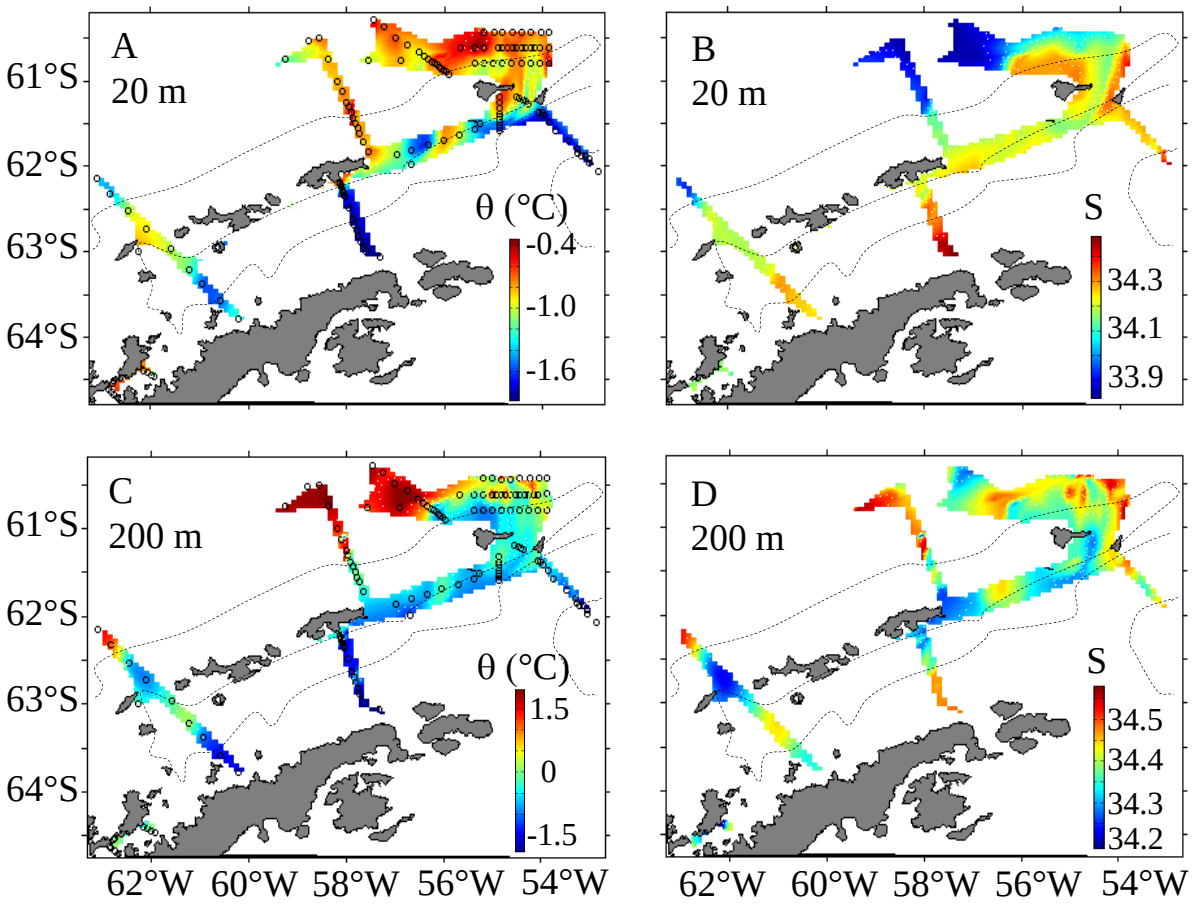

Fig. 2. Horizontal distributions of potential temperature (θ) at 20 m (A), salinity (S) at 20 m (B), θ at 200 m (C), and S at 200 m (D). The thin dash lines are the 500 m isobath.

Fig. 02

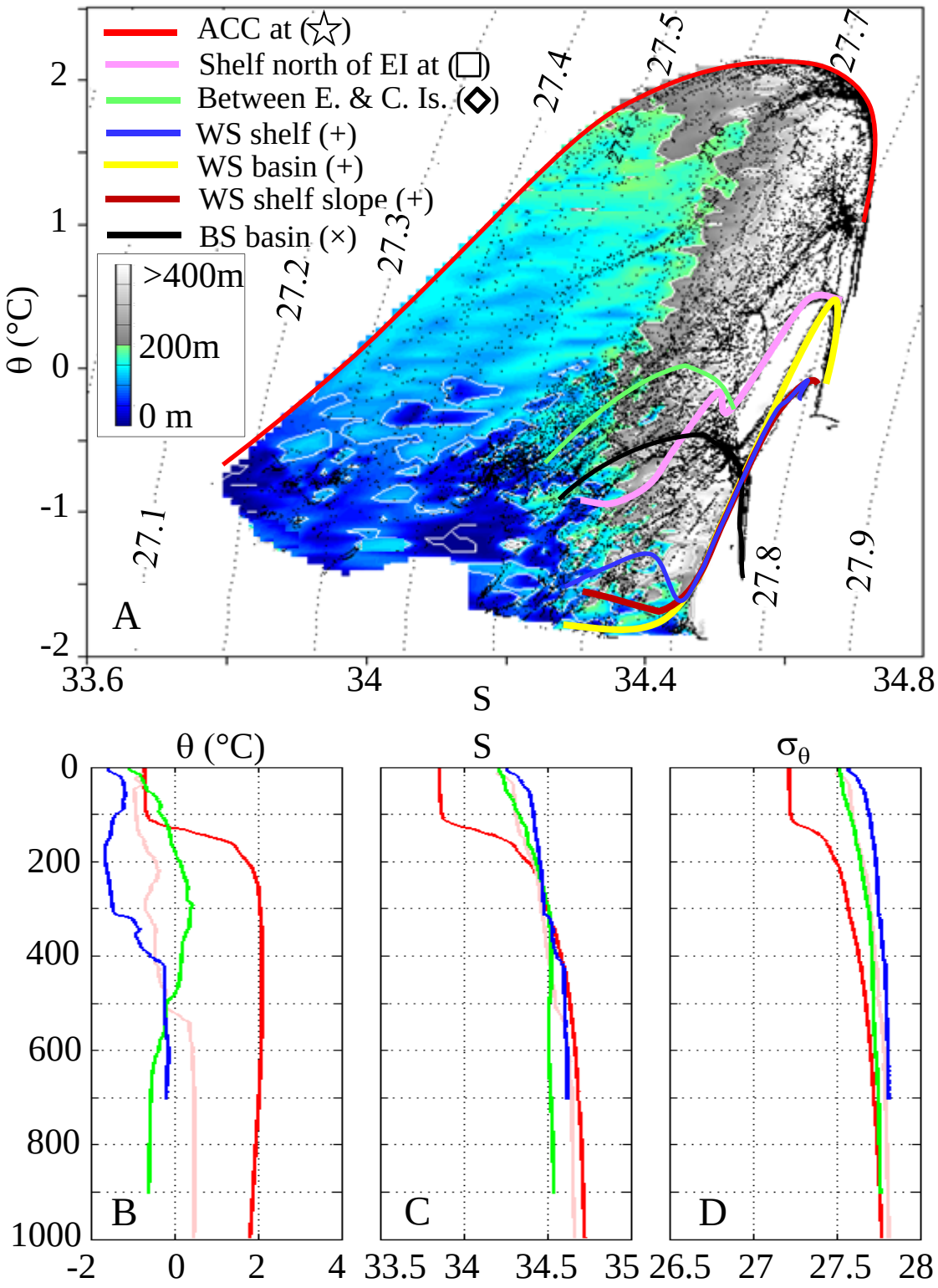

Fig. 3. θ-S diagrams (A) and vertical profiles of θ (B), S (C) and potential density (σ_θ) (D) for the typical water types in the study area. In panel A, the small black dots are all θ–S pairs in our survey area, color coded solid lines represent the θ-S diagrams and vertical profiles of waters in the ACC shelf, Bransfield Current, Bransfield Strait basin and Weddell Sea basin regions, the dashed lines are the surface σ_θ contours, and the color and gray scales represent the depths of θ-S pairs.

Fig. 03

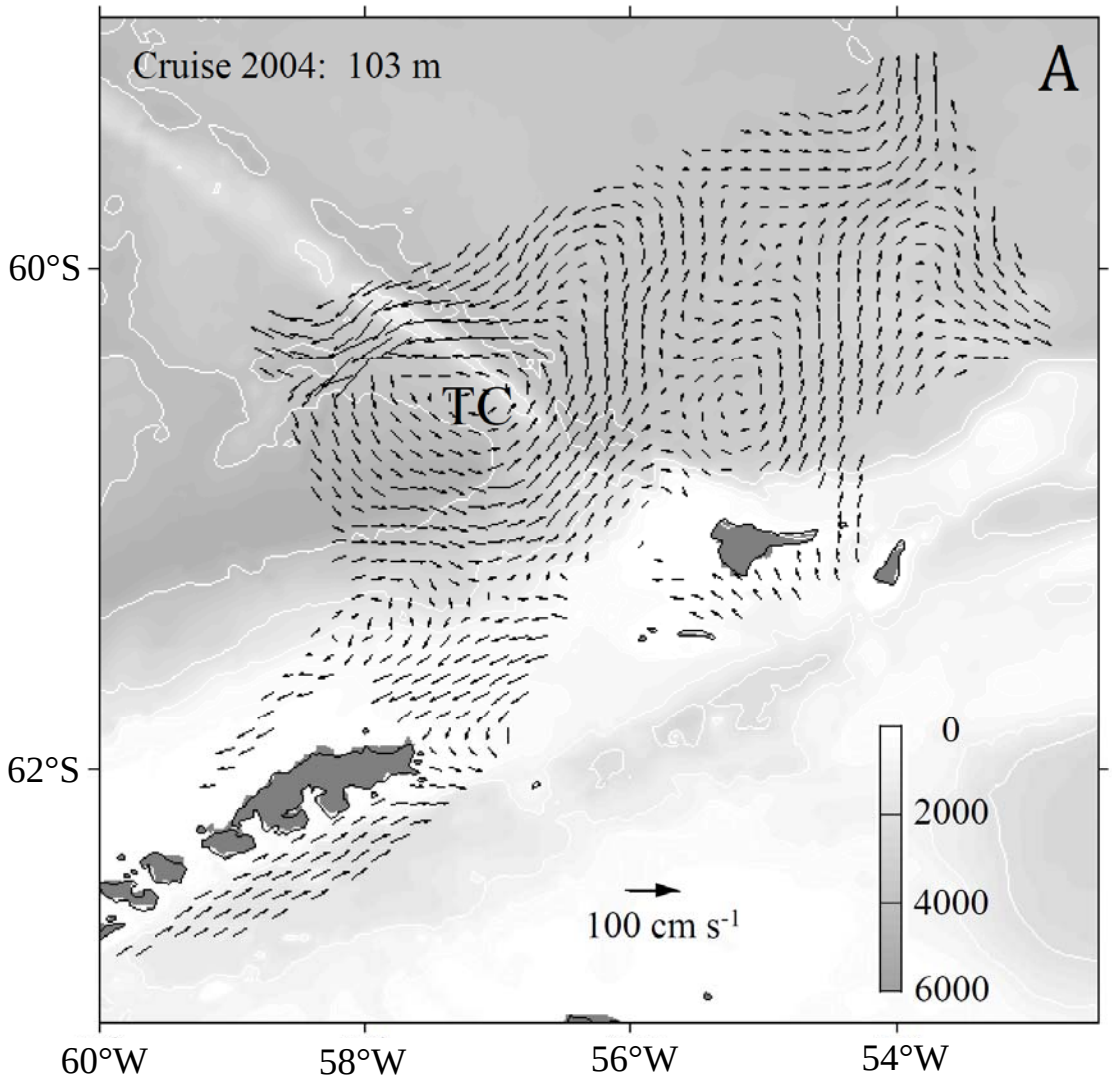

Fig. 4. Circulation field at 103 m (A), and 199 m (B) based on ADCP current measurements during the 2004 austral summer cruise. The current field was interpolated based on the least-squares streamfunction fitting. The Taylor Column is marked by "TC."

Fig. 04A

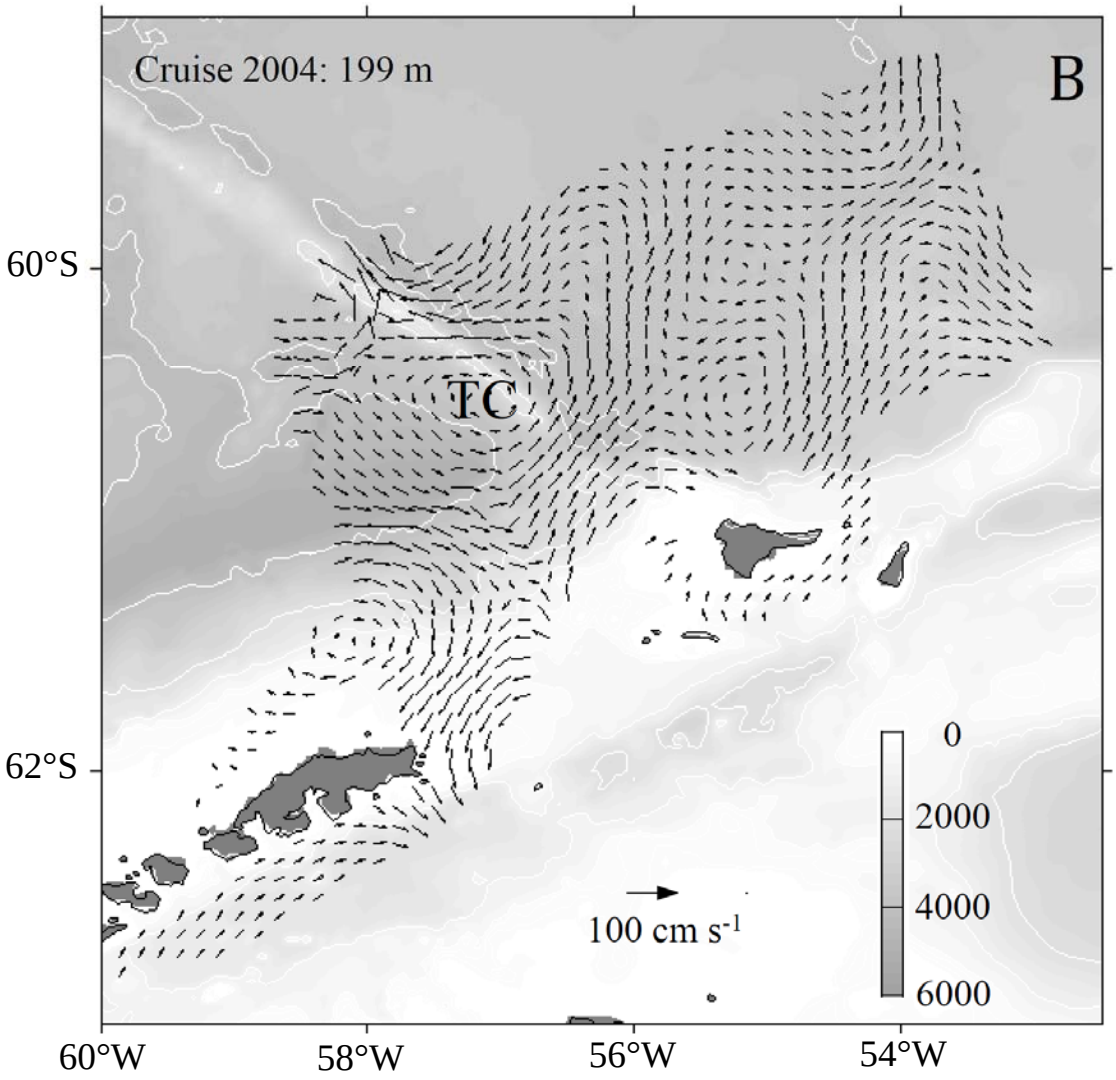

Fig. 4. Continued

Fig. 04B

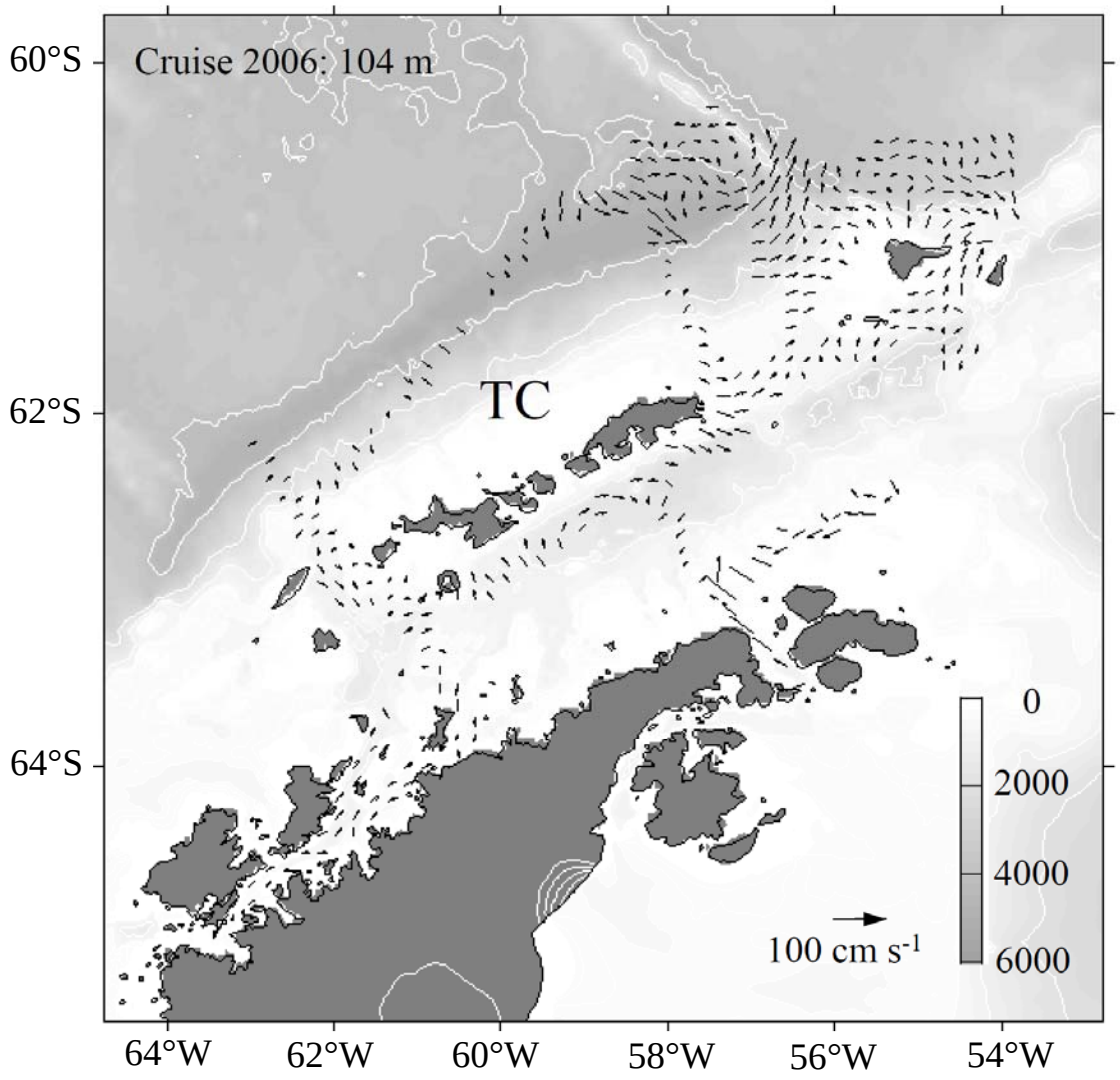

Fig. 5. Circulation field at 104 m based on ADCP current measurements during the 2006 austral winter cruise. The current field was interpolated based on the least-squares streamfunction fitting.

Fig. 05

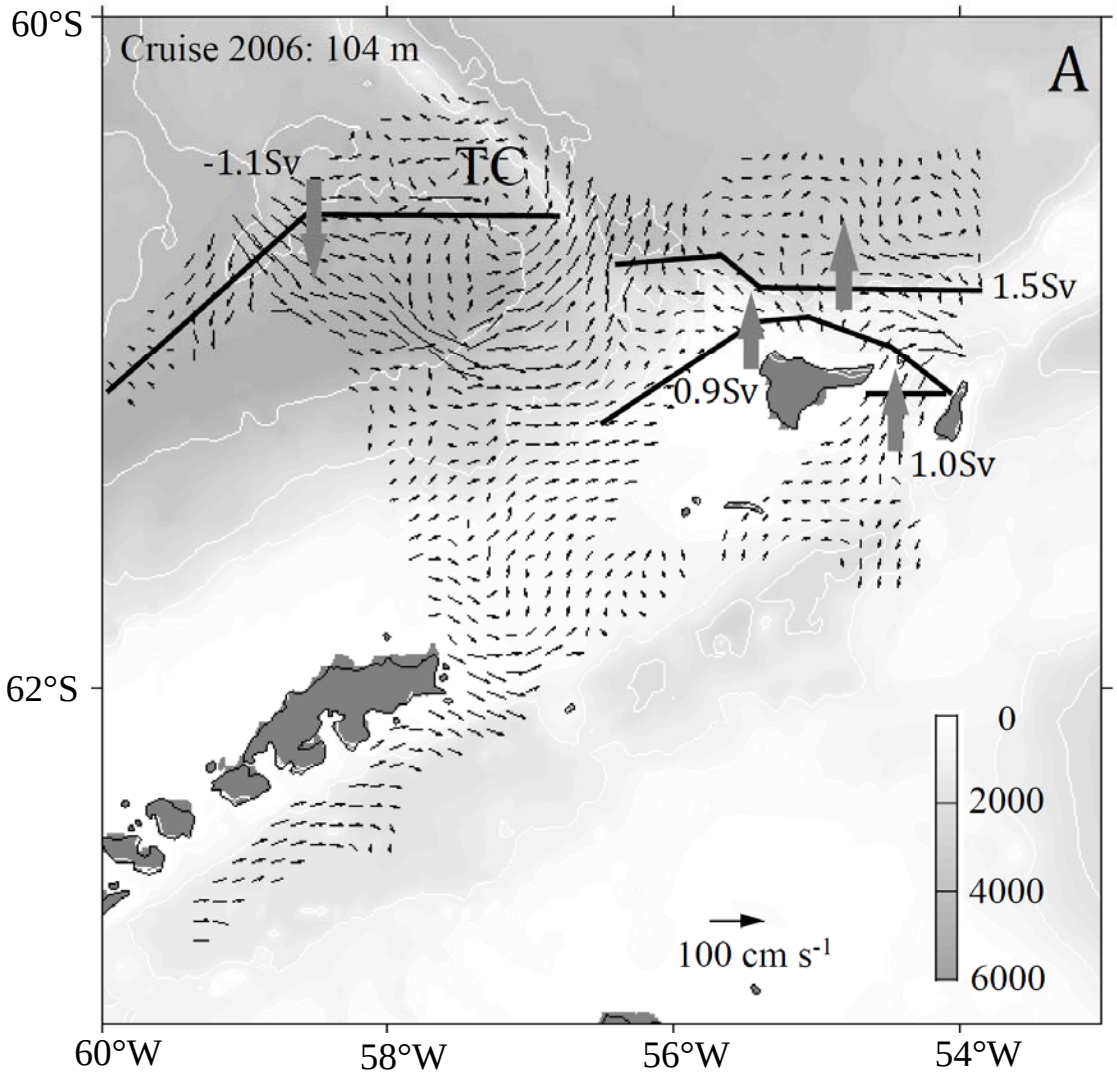

Fig. 6. Circulation field at 104 m (A), and 200 m (B) based on ADCP current measurements during the 2006 austral winter cruise. The current field was interpolated based on the least-squares streamfunction fitting. The black solid lines indicate where the northward transport is estimated from direct ADCP current measurements, and values are the estimates of northward transport in the upper 200 m.

Fig. 06A

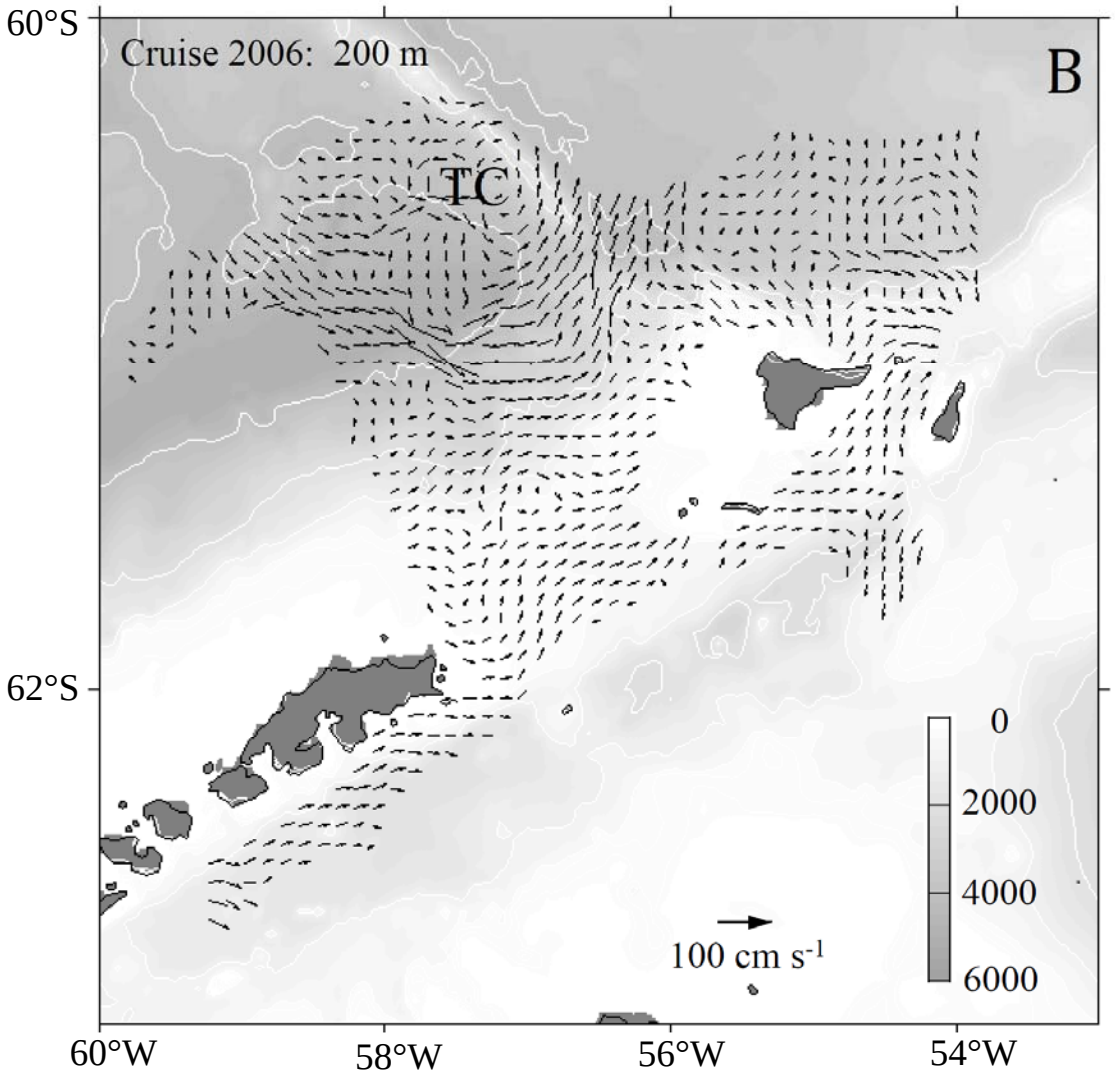

Fig. 6. Continued

Fig. 06B

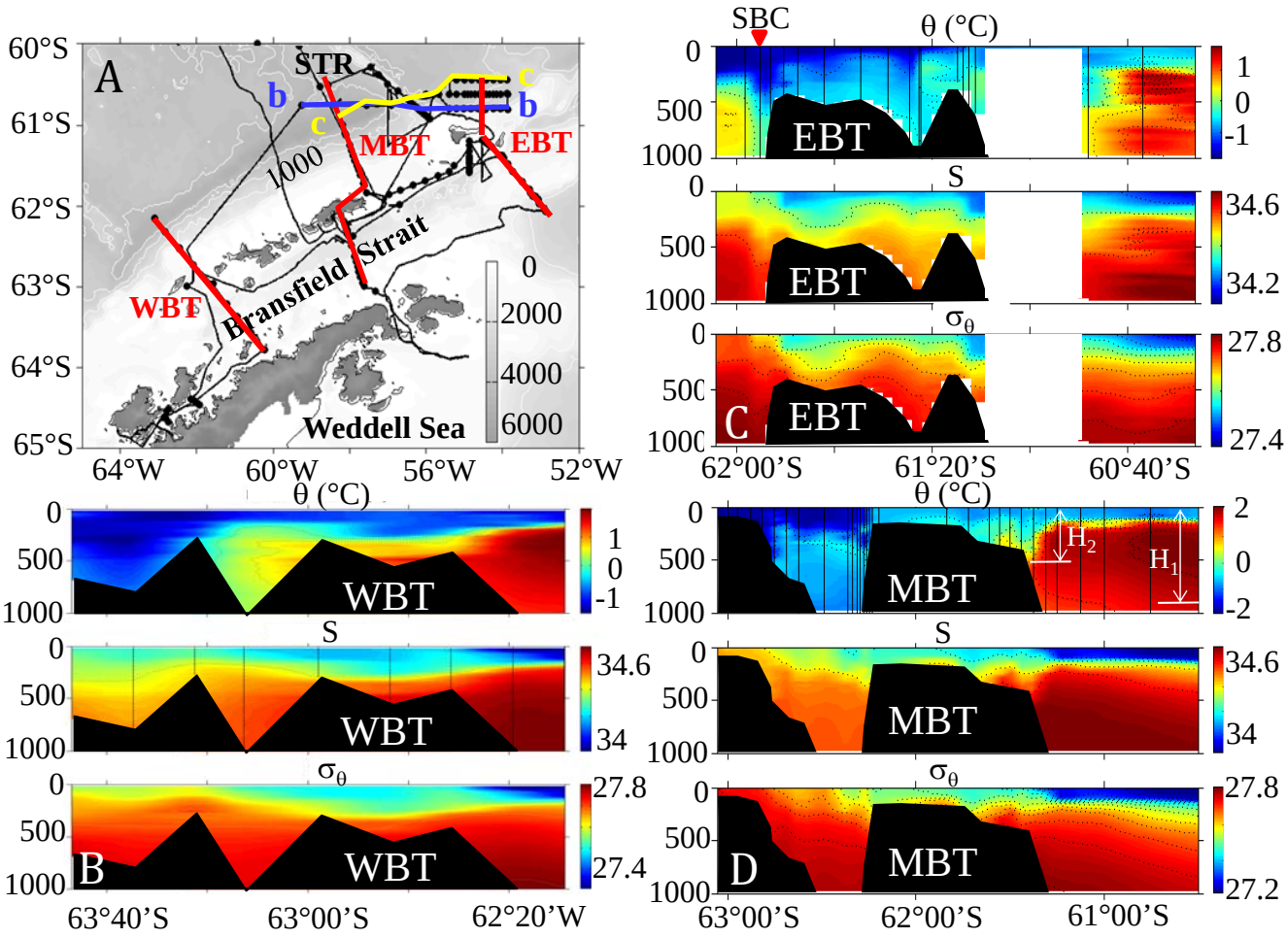

Fig. 7. Locations of the transects showed in Figs. 7-9 (A), and transects of θ (B), S (C) and σ_θ (D) along 3 south-north red lines marked by WBT, EBT and MBT in panel A. In panels B)-D, the vertical black lines indicate the locations and depths of CTD casts, and contour intervals are 0.5 °C, 0.2 and 0.05 for θ, S and σ_θ, respectively. In panel A, the blue solid line marked by b-b indicates the location of the transect shown in Fig. 8, and the yellow solid line marked by c-c indicates the location of the transect shown in Fig. 9. In panel C, SBC marks the location of the shelf break current at the Weddell Sea shelf slope.

Fig. 07

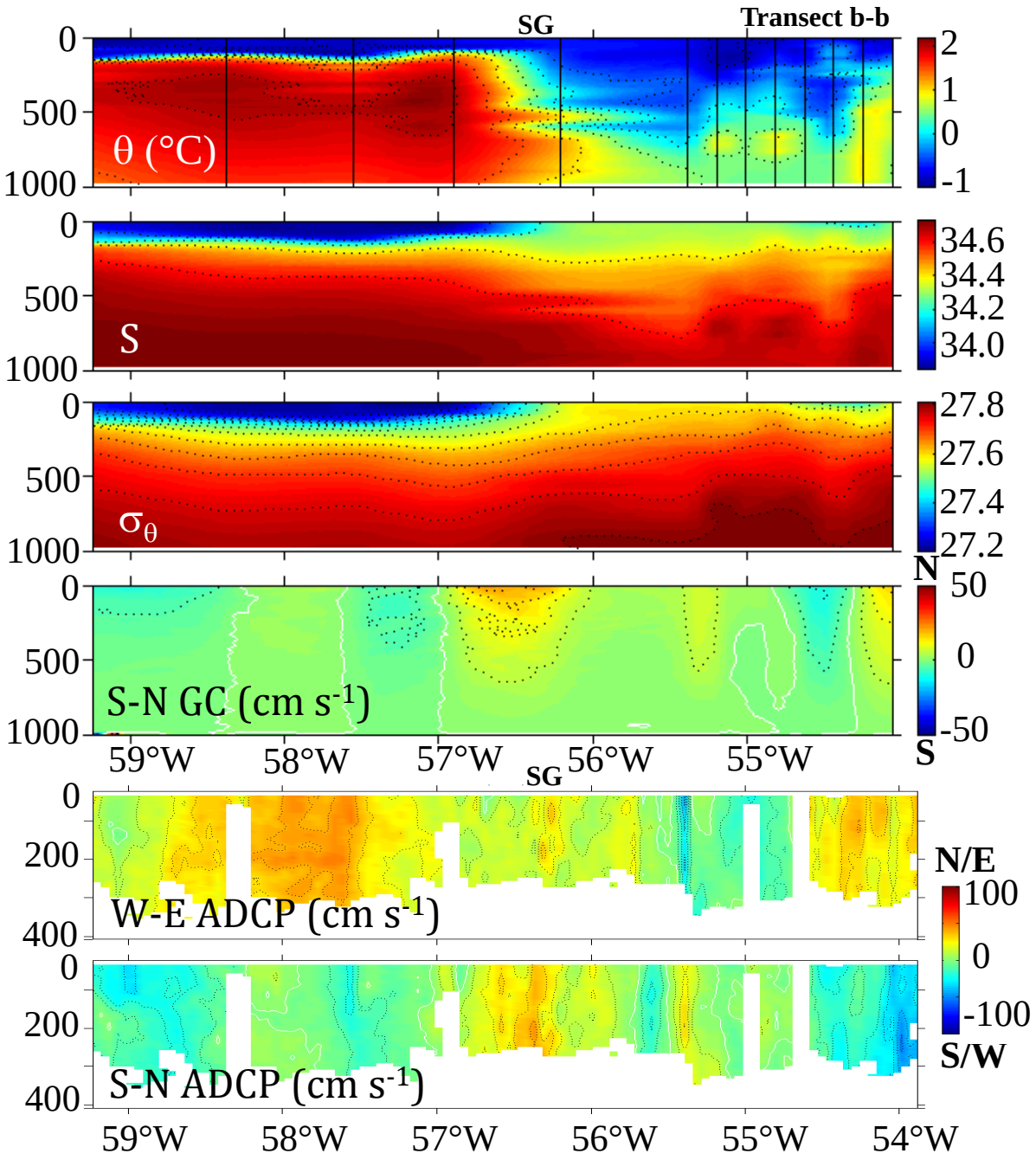

Fig. 8. Transects of θ, S, σ_θ, geostrophic current estimates relative to 1000 m, west-east (W-E) component of ADCP current measurements, and S-N component of ADCP current measurements along line b-b indicated in Fig. 7. The vertical black lines indicate the locations and depths of CTD casts, contour intervals are 0.5 °C, 0.2, 0.05 and 5 cm s^{-1} for θ, S, σ_θ and currents, respectively, and SG marks the location of the Shacklton Gap.

Fig. 08

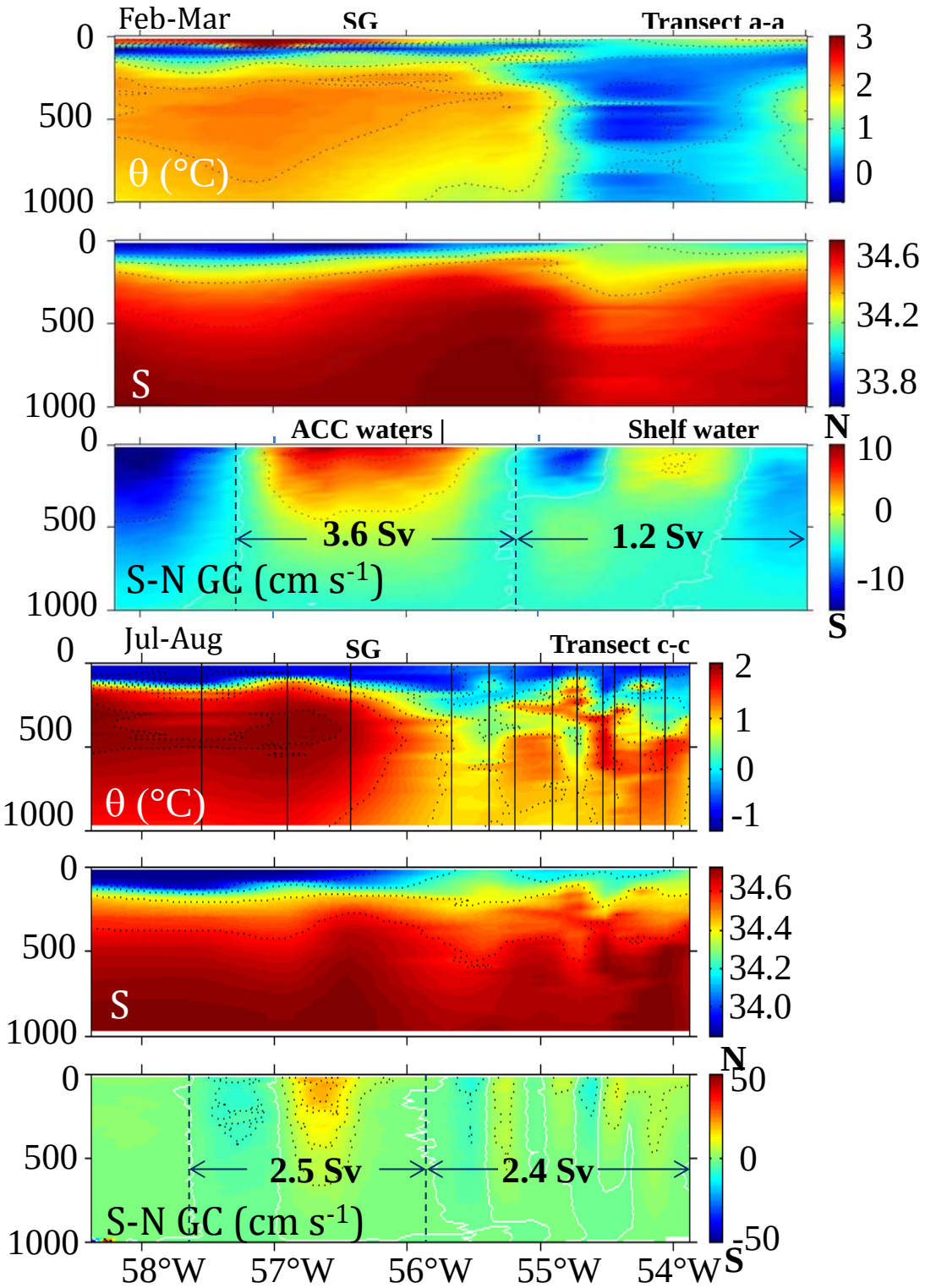

Fig. 9. Transects of θ, S and geostrophic current estimates relative to 1000 m along lines a-a and c-c in the 2004 and 2006 cruises, respectively. The locations of these transects are shown in Figs. 1 and 7. The values inserted in the geostrophic current panels are the positive northward transport estimates in Sv within the sections indicated by dashed lines. The vertical black lines indicate the locations and depths of CTD casts and contour intervals are 0.5 °C, 0.2 and 5 cm s^{-1} for θ, S and currents, respectively.

Fig. 09

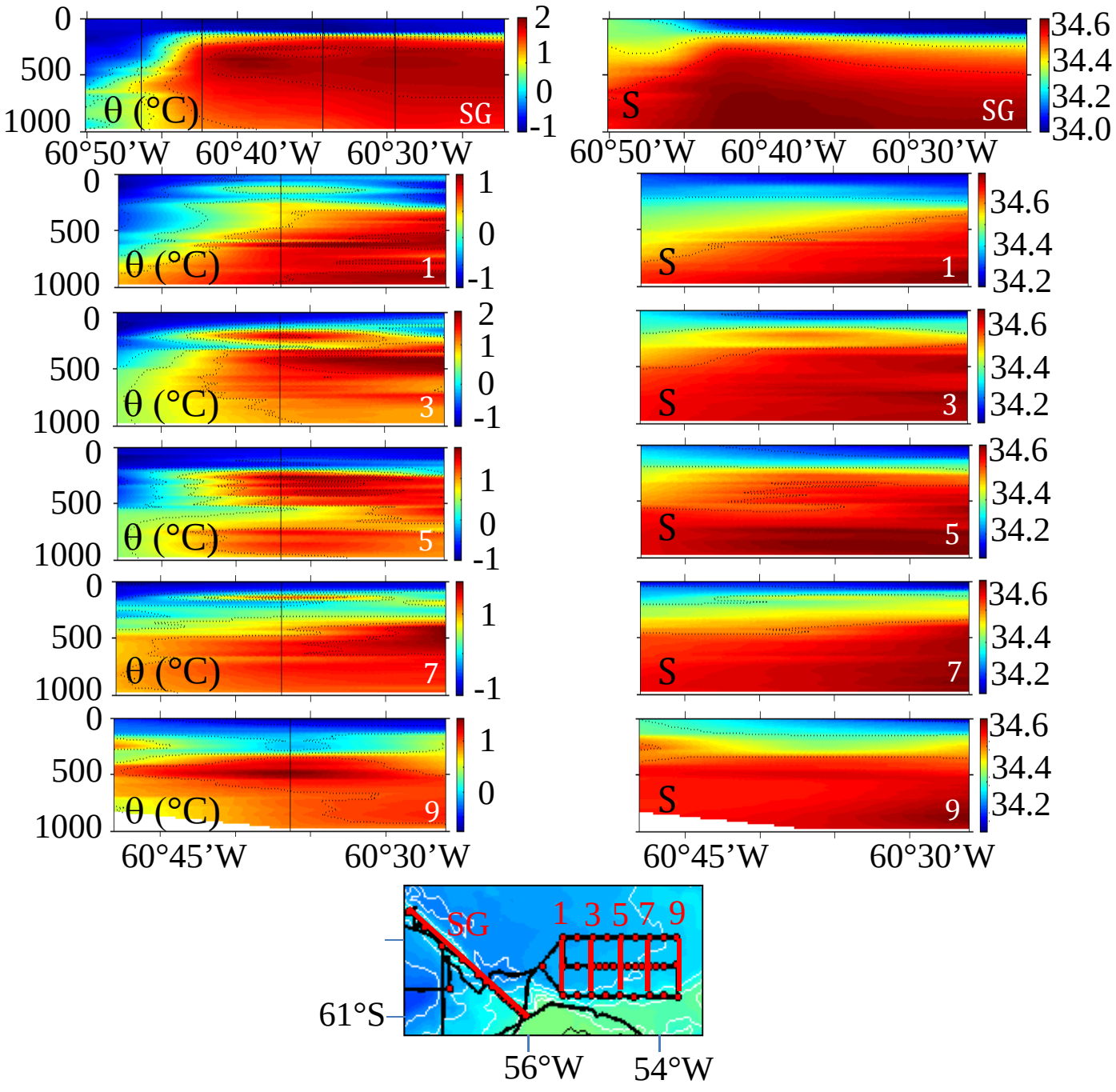

Fig. 10. Transects of θ and S along lines SG and 1-9 shown in the inserted panel during the 2006 cruise. The vertical black lines indicate the locations and depths of CTD casts and contour intervals are 0.5 °C and 0.2 for θ and S, respectively.

Fig. 10

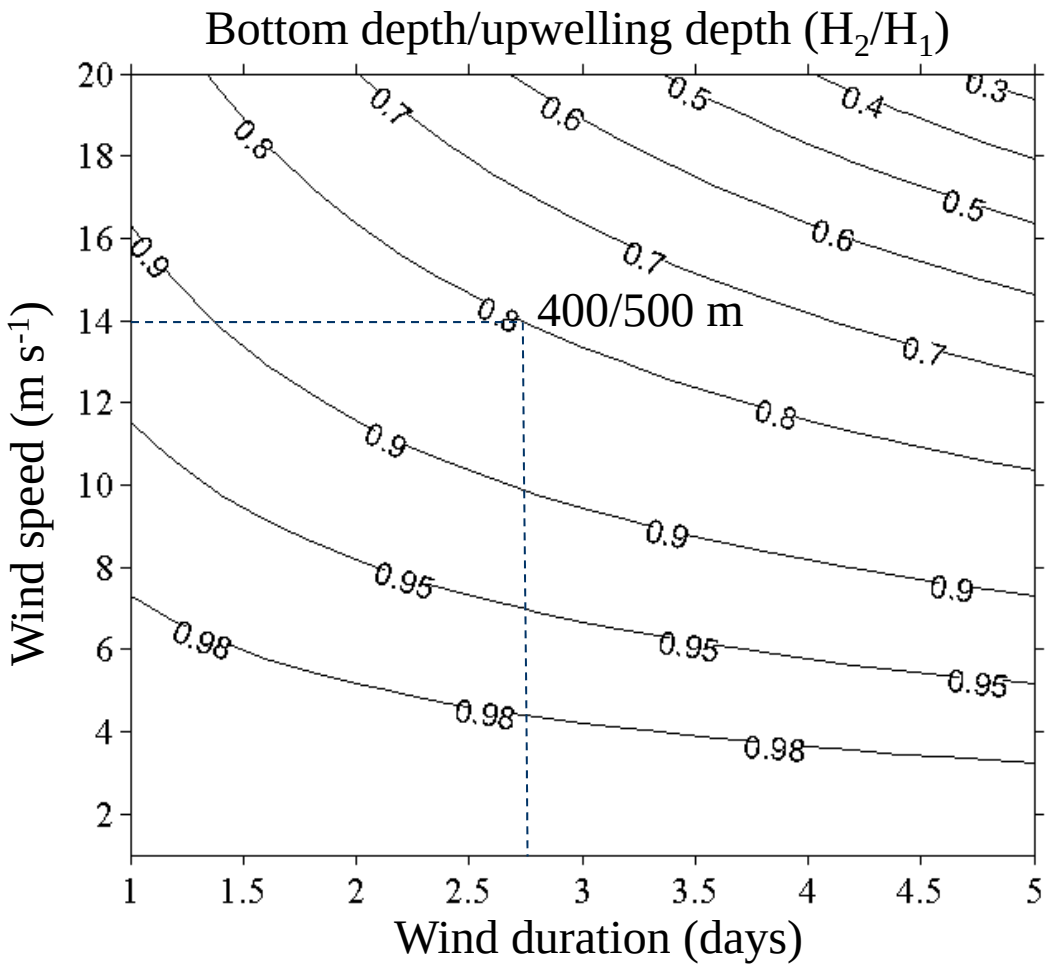

Fig. 11. Predicted relationship between the ratio of a shelf bottom depth (H_2) to the original depth (H_1) of upwelled CDW, wind speed and wind duration. The dashed lines show the example of a 14 m s^{-1} wind would take 2.75 days to raise a water mass at 500 m off the shelf break to a shelf bottom depth of 400 m.

Fig. 11

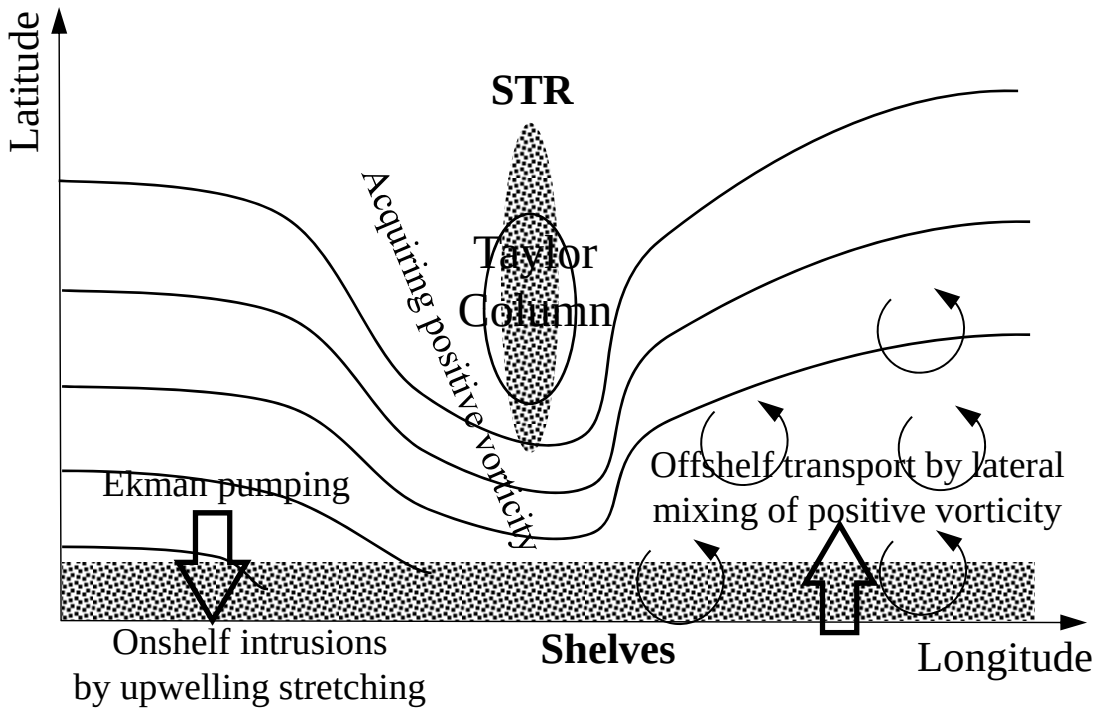

Fig. 12. Plan view of a conceptual configuration of the geophysical fluid dynamic processes in the southern Drake Passage: To the west of the STR, a westerly wind event produces upwelling and stretching of water column that leads to intrusions of the CDW onto the shelf; the blockage of the ACC by the STR produces a Taylor Column and the southward detouring of an ACC branch; the ACC waters that intrude onto the shelf acquire a positive vorticity due to the β-effect and are horizontally mixed with shelf waters leading to a northward offshelf transport.

Fig. 12